

Review

Review on Mono and Hybrid Nanofluids: Preparation, Properties, Investigation, and Applications in IC Engines and Heat Transfer

Atul Bhattad ¹, Vinay Atgur ¹, Boggarapu Nageswar Rao ¹, N. R. Banapurmath ^{2,3,*}, T. M. Yunus Khan ⁴, Chandramouli Vadlamudi ⁵, Sanjay Krishnappa ⁵, A. M. Sajjan ^{3,6}, R. Prasanna Shankara ⁷ and N. H. Ayachit ³

¹ Department of Mechanical Engineering, Koneru Lakshmaiah Education Foundation, Vaddeswaram 522302, India

² Department of Mechanical Engineering, K.L.E. Technological University, Hubballi 580031, India

³ Centre of Excellence in Material Science, K.L.E. Technological University, Hubballi 580031, India

⁴ Mechanical Engineering Department, College of Engineering, King Khalid University, P.O. Box 394, Abha 61421, Saudi Arabia

⁵ Aerospace Integration Engineer, Aerosapien Technologies, Daytona Beach, FL 32114, USA

⁶ Department of Chemistry, K.L.E. Technological University, Hubballi 580031, India

⁷ Department of Mechanical Engineering, Yenepoya Institute of Technology, Mangalore 574225, India

* Correspondence: nr_banapurmath@kletech.ac.in; Tel.: +91-0836-2378295

Abstract: Nano fluids are widely used today for various energy-related applications such as coolants, refrigerants, and fuel additives. New coolants and design modifications are being explored due to renewed interest in improving the working fluid properties of heat exchangers. Several studies have investigated nanofluids to enhance radiator and heat exchanger performance. A new class of coolants includes single, binary, and tertiary nanoparticle-based hybrid nano-coolants using ethylene glycol/deionized water combinations as base fluids infused with different nanoparticles. This review article focuses on the hydrothermal behavior of heat exchangers (radiators for engine applications) with mono/hybrid nanofluids. The first part of the review focuses on the preparation of hybrid nanofluids, highlighting the working fluid properties such as density, viscosity, specific heat, and thermal conductivity. The second part discusses innovative methodologies adopted for accomplishing higher heat transfer rates with relatively low-pressure drop and pump work. The third part discusses the applications of mono and hybrid nanofluids in engine radiators and fuel additives in diesel and biodiesel blends. The last part is devoted to a summary of the research and future directions using mono and hybrid nanofluids for various cooling applications.

Keywords: nanofluids; heat transfer rate; Prandtl number; pressure drop; IC engines



Citation: Bhattad, A.; Atgur, V.; Rao, B.N.; Banapurmath, N.R.; Yunus Khan, T.M.; Vadlamudi, C.; Krishnappa, S.; Sajjan, A.M.; Shankara, R.P.; Ayachit, N.H. Review on Mono and Hybrid Nanofluids: Preparation, Properties, Investigation, and Applications in IC Engines and Heat Transfer. *Energies* **2023**, *16*, 3189. <https://doi.org/10.3390/en16073189>

Academic Editor: Abdalnaser Sayma

Received: 20 February 2023

Revised: 15 March 2023

Accepted: 30 March 2023

Published: 31 March 2023



Copyright: © 2023 by the authors. Licensee MDPI, Basel, Switzerland. This article is an open access article distributed under the terms and conditions of the Creative Commons Attribution (CC BY) license (<https://creativecommons.org/licenses/by/4.0/>).

1. Introduction

One of the dominant threats in the current energy scenario is the depletion of energy reserves. Thermal systems such as refrigerators, heat pumps, and air conditioners place enormous energy demands. Due to limited energy resources, several investigations have been conducted to improve thermal system efficiency and performance by reforming the design of system components or changing the working fluid. Many small heating devices (such as tube heat exchangers, plate heat exchangers, and mini-channel heat exchangers) with mono/hybrid nanofluid usage improve the system's performance.

1.1. Heat Exchanger

Heat exchangers (HEs) play an essential role in thermal energy management. Regarding the energy crisis, efficient HEs are needed to develop new energy-efficient technologies for industries to reduce energy consumption. Therefore, researchers are focusing on improving the design of equipment and the thermal properties of working fluids. Energy

optimization also becomes very important due to the limitations associated with conventional fuels. Energy savings can be achieved by increasing the performance of HEs. HEs available are plate-type heat exchangers (PHEs), double-pipe heat exchangers (DPHEs), heat pipes (HPs), and mini-channel/heat sinks (Figure 1). Because of compactness, high effectiveness, flexibility, ease of handling, and high thermal performance, PHEs originated to meet the requirements of the dairy industries and other engineering applications (such as heat recovery, HVAC, cooling, offshore oil, breweries, power generation, dairy, food processing, chemical, pulp and paper production, and refrigeration). In DPHEs, both fluids can move in the same or opposite directions [1]. Power plants use shell-and-tube or double-pipe HEs to generate electricity. Heaters and economizers are components of these plants [2]. DTHEs have become widespread in use due to their simple design, easy cleaning, and low cost involved [3]. Portable devices (laptops, mobile phones, etc.) are preferable, which require limited space. Cooling these small objects is a challenge. Thus, mini/micro channels have emerged [4]. HPs also play an essential role in cooling these small devices [5]. Improved heat transfer in HEs is accompanied by higher pumping power. Therefore, the benefit of enhanced heat transfer and associated pressure loss must be balanced [6].

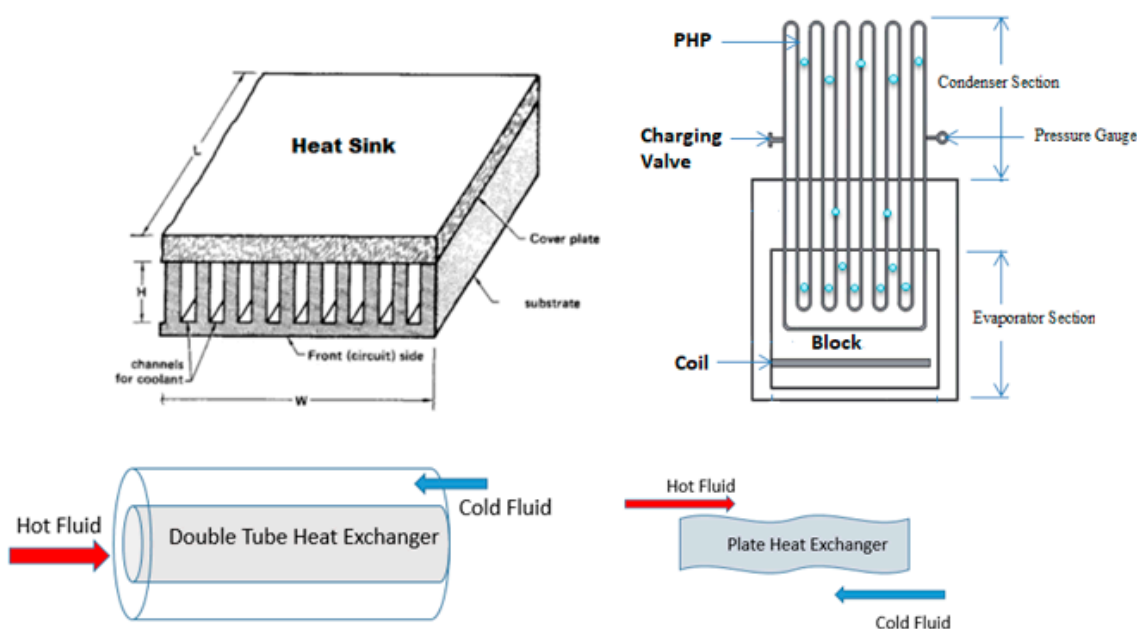


Figure 1. Heat exchangers.

1.2. Hybrid Nanofluids

Industries with cooling solution requirements have focused on the use of modified fluids with various additives [7] to obtain improved thermal properties. Nanofluids are colloidal mixtures of nanosized particles (10–100 nm) suspended in base fluids [8]. They possess good physical or chemical properties and thermal or rheological properties [9,10]. Hybrid nanofluids are suspensions of a mixture of dissimilar nanoparticles or nanocomposites infused in the conventional base fluid, which yield better thermal conductivity and heat transfer characteristics due to hybridization [11]. They are used in phase change materials, heat exchangers, solar energy, electronics, agriculture, chemical, manufacturing, and automobile industries [12–25]. The two-step method is used for preparing hybrid nanofluids. Different nanoparticles are prepared and mixed in the primary liquid through magnetic or mechanical stirring. The solution is sonicated and characterized to ensure stable and homogeneous mixing, providing improved heat transfer characteristics [26]. Enhanced heat transfer is due to increased surface area, collision, interactive effect, and proper mixing of nanoparticles in base fluids (causing micro turbulences). Hybrid nanofluids play four roles (used as refrigerant, lubricant, absorbent, and secondary refrigerant) in improving the

thermal system performance in low-temperature applications. The effects of nanoparticle concentration and size on the performance of water-based CuO nanofluids were investigated in [27]. The synthesis, stability, and thermo-physical properties of hybrid nanofluids were studied in [28]. Zaynon and Azmi [29] presented the influence of nanoparticle type, concentration, temperature, shape, and size on the nanofluid properties. The amount of grapheme required in the base fluid to improve thermal performance was suggested in [30].

1.3. Secondary Refrigerant

Global warming has been a significant concern for environmentalists during the past couple of decades. Refrigeration industries replaced chlorofluorocarbons (CFCs) and hydrochlorofluorocarbons (HCFCs) with hydrofluorocarbons (HFCs) to overcome the ozone depletion problem. Supermarket refrigeration systems utilize direct expansion systems with separate evaporation units. Up to 30% loss of refrigerant charges is estimated annually [31]. This refrigerant charge leak exacerbates the global warming problem. There is a necessity for a secondary refrigerant to reduce the leak. Liquid cooling systems are used in industrial refrigeration and commercial air conditioning [32]. A secondary circuit cooling system uses primary and secondary refrigerants. The primary refrigerant (while undergoing a phase change in the evaporator) cools the secondary pumping fluid to the supermarket for cooling. Secondary refrigerants minimize the leakage of primary refrigerants with the possibility of load sharing and easy maintenance. They improve the thermophysical properties of the primary refrigerants, overcoming the additional investment cost and pump work requirement.

1.4. Objectives

The remainder of this review describes the hydrothermal characteristics of a nanofluid-driven single/hybrid plate heat exchanger (PHE), covers the creation of hybrid nanofluids, the empirical relationship with thermo-physical properties, and innovative ways to achieve high heat transfer with relatively low-pressure drops, as well as the research on using single and hybrid nanofluids for heat exchangers (HE) and internal combustion engines (ICEs), and highlights the potential for using single and hybrid nanofluids in the low-temperature sector.

2. Preparation of Mono/Hybrid Nanofluids

Nanofluids are organized according to their preparation using one- or two-step methods (Figure 2). In a one-step approach, nanoparticles are prepared and mixed directly in a base fluid using physical or chemical processes. In the two-step method, nanoparticles are obtained using physical or chemical methods and then effectively infused in an essential base liquid [33]. Several investigators have reviewed the preparation of different mono/hybrid nanofluids based on various base fluids [34–44]. Spherical ZnO particles were synthesized using a sol–gel annealing process at 500–600 °C in [45]. The ball milling process was used to grind aluminum nitride carbon nanocomposite (a nontoxic ceramic) for heat transfer experiments [46]. Making nanofluids through a single-step method is expensive and time-consuming. The control of particle agglomeration is the primary problem in the two-step method. Ultrasonication minimizes nanoparticle sedimentation and improves nanofluid stability [47]. Due to simplicity, 95% of researchers used a two-step method when preparing nanofluids (see Table 1).

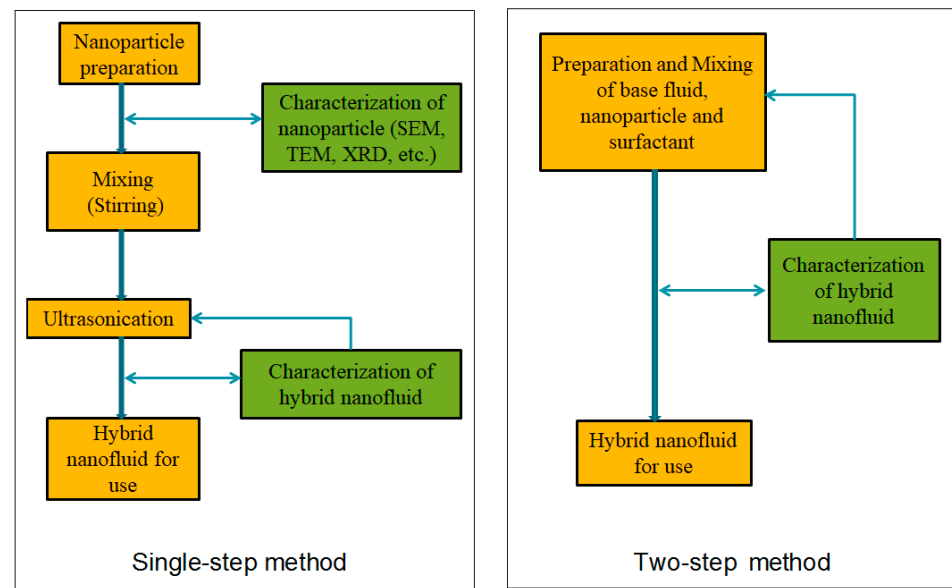


Figure 2. Flowchart for producing hybrid nanofluids [48].

Table 1. Examples of hybrid nanofluids adopting two-step preparation.

Author(s)	Nanoparticle	Base Fluid
Jana et al. [49]	Au–CNT, Cu–CNT	Water
Han et al. [50]	Sphere–CNT	Oil
Turcu et al. [51]	Fe ₃ O ₄ –polypyrrole	Water
Jha and Ramaprabhu [52]	Cu–MWCNT	Water/EG
Han and Rhi [53]	Ag–Al ₂ O ₃	Water
Baby and Sundara [54]	CuO–HEG	Water/EG
Paul et al. [55]	Al–Zn	EG
Suresh et al. [56]	Al ₂ O ₃ –Cu	Water
Botha et al. [57] *	Ag–SiO ₂	Oil
Ho et al. [58]	Al ₂ O ₃ –PCM	Water
Baby and Sundara [59]	Ag–HEG	Water/EG
Amiri et al. [60]	Ag–MWCNT	Water
Chen et al. [61]	Ag–MWCNT	Water
Aravind and Ramaprabhu [62]	Graphene–MWCNT	Water and EG
Bhosale and Borse [63]	Al ₂ O ₃ –CuO	Water
Balla et al. [64]	CuO–Cu	Water
Abbasi et al. [65]	Y–Al ₂ O ₃ –MWCNT	Water
Nine et al. [66]	Cu–Cu ₂ O	Water
Munkhbayar et al. [67] *	Ag–MWCNT	Water
Sundar et al. [68]	Nanodiamond–nickel	Water/EG
Parameshwaran et al. [69]	Ag–TiO ₂	PCM
Batmunkh et al. [70]	Ag–TiO ₂	Water
Madhesh et al. [71]	Cu–TiO ₂	Water

Table 1. Cont.

Author(s)	Nanoparticle	Base Fluid
Chen et al. [72]	MWCNT-Fe ₃ O ₄	Water
Parekh [73]	Mn _{0.5} Zn _{0.5} Fe ₂ O ₄	Oil
Luo et al. [74]	Al ₂ O ₃ -TiO ₂	Lubricating oil
Madhesh and Kalaiselvam [75]	Cu-TiO ₂	Water
Zubir et al. [76]	Graphene oxide-CNT	Water
Qadri et al. [77]	Graphene-Cu ₂ O	Water/EG
Karimi et al. [78]	NiFe ₂ O ₄	Water
Chakraborty et al. [79]	Cu-Al	Water
Megatif et al. [80]	CNT-TiO ₂	Water
Abbasi et al. [81]	MWCNT-TiO ₂	Water
Toghraie et al. [82]	ZnO-TiO ₂	EG
Bhanvase et al. [83]	PANI-CuO	Water
Asadi et al. [84]	CuO-TiO ₂	Water
Chen et al. [85]	Al ₂ O ₃	Liquid paraffin
Asadi et al. [86]	MWCNT	Water
Gulzar et al. [87]	Al ₂ O ₃ -TiO ₂	Therminol-55
Alarifi et al. [88]	MWCNT-TiO ₂	Oil
Akram et al. [89]	CGNP	DI Water
Sharafeldin and Grof [90]	WO ₃	Water
Chen et al. [91]	MWCNT	Water
Ali et al. [92]	Al	Water
Mahbubul et al. [93]	Al ₂ O ₃	Water
Mahyari et al. [94]	GO-SiC	Water/EG
Chen et al. [95]	Fe ₃ O ₄ -MWCNT	Brine water
Okonkwo et al. [96]	Al ₂ O ₃ -Fe	Water
Terueal et al. [97]	MoSe ₂	Water
Li et al. [98]	SiO ₂	Liquid paraffin
Geng et al. [99]	ZnO-MWCNT	Oil
Li et al. [100]	SiO ₂	EG

* Single-step method.

Jana et al. [49] infused various volume fractions of CNTs in water to obtain CNT suspensions. Au nanoparticles were suspended with CNT in varying volume fractions to obtain CNT-Au suspensions. The hybrid suspension was sonicated for 1 h using an ultrasonic cleaner to get an adequately dispersed solution. Bhosale and Borse [63] prepared a hybrid nanofluid (Al₂O₃-CuO water) by mixing 2.5 mg of CuO and Al₂O₃ in distilled water. Later, the concentration was varied to 0.25%, 0.5%, and 1.0% volume. Toghraie et al. [82] prepared ZnO-TiO₂/EG hybrid nanofluids by dispersing equal volumes of ZnO and titanium dioxide (TiO₂) nanoparticles in a given amount of pure EG as a base liquid. The stability of the prepared nanofluid was confirmed, ensuring no sedimentation. Paul et al. [55] synthesized Al-Zn nanoparticles by stirring. They prepared hybrid nanofluids through a two-step process. Al-Zn nanoparticles were added to ethylene glycol (base fluid), followed by sonication and magnetic stirring. Suresh et al. [56] obtained a hybrid powder of alumina-copper using a thermochemical method, including spray-drying, ox-

idation of the precursor powder, hydrogen reduction, and homogenization. They used different volume fractions (0.1%, 0.33%, 0.75%, 1.0%, and 2.0%). Baby and Sundara [54] used a hydrogen-induced exfoliation and chemical reduction process of graphite oxide (GO) to synthesize graphene decorated with CuO (CuO/HEG). The HEG obtained was functionalized by acid treatment and coated with CuO nanoparticles. CuO/HEG was dispersed in the base liquid (water/EG) by ultrasonication. Nine et al. [66] reported an economical and beneficial process for synthesizing Cu₂O and Cu/Cu₂O nanoparticles with a mean size of less than 30 nm. A ball milling process was used to synthesize Cu/Cu₂O–water hybrid nanofluids. Madhesh et al. [71] prepared a copper–titania hybrid nanofluid by uniformly dispersing an aqueous solution of titania (5 g) and copper acetate (0.5 g) in an ultrasonic vibrator for 2 h using reducing agents at 45 °C and atmospheric pressure. A one-step method was described for a hybrid nanofluid containing silver and silica nanoparticles by Botha et al. [57]. Ho et al. [58] prepared phase change material (PCM) suspensions using interfacial poly-condensation and emulsion techniques. Nanofluid Al₂O₃–water was obtained by adding Al₂O₃ nanoparticles in water (base liquid). Chen et al. [61] prepared Ag/MWCNT nanocomposites using the silver mirror reaction. Functionalized MWCNTs were used to fabricate Ag/MWCNT nanocomposites using sodium dodecyl sulfate (SDS) as a surfactant and formaldehyde as a reducing agent.

3. Characterization and Stability of Mono/Hybrid Nanofluids

Several forces, such as van der Waals attraction, buoyancy, gravity, and electrostatic repulsion, cause destabilization and sediment formation. Van der Waals attraction and gravity decrease the stability of colloidal suspensions. Stability is a critical factor in the effectiveness of nanofluids for technological applications. All thermo-physical properties of nanofluids depend on their stability. The instability of nanofluids can reduce their effectiveness in many heat transfer applications. It is caused by the tendency of nanoparticles to form clusters in liquids. An SEM image of the Al₂O₃–MWCNT/water hybrid nanofluid is shown in Figure 3 [101].

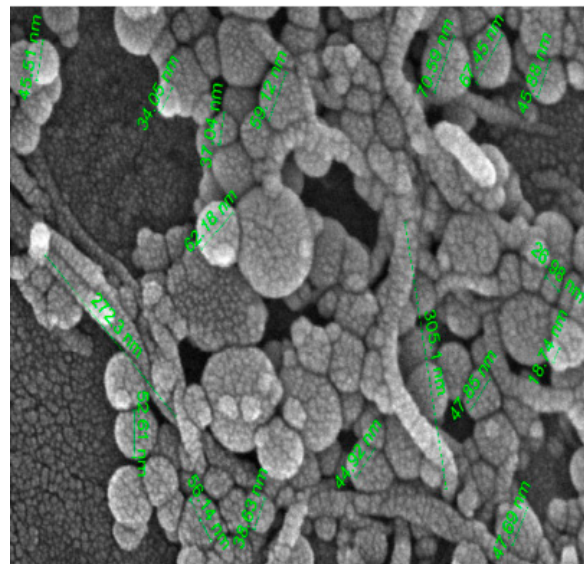


Figure 3. SEM image of Al₂O₃–MWCNT/water hybrid nanofluid [101].

The particle aggregation causes the separation of nanoparticles from base fluids and forms sedimentation [102]. The coagulation rate is determined from the collision frequency of particles in Brownian motion and cohesion probability [103]. Removal of agglomeration propensity yields stable nanofluids. Methods adopted for assessing the stability of nanofluids are the sedimentation method, spectral absorbance, centrifugation method, transmittance measurement, zeta potential measurement, and dynamic light

scattering [104]. For long-term stable and homogenous nanofluids, the following surfactants can be added [105,106]: anionic (sodium dodecyl sulfate and sodium dodecyl benzene sulfonate), cationic (cetyl trimethyl ammonium bromide), nonionic (Span-80 and Tween-20), and polymer (polyvinyl pyrrolidone, polyvinyl alcohol, and gum Arabic). Surfactants improve the wettability of the nanoparticles and the base fluids by reducing the base fluid's surface tension and improving the nanoparticles' dispersibility [107].

Ultrasonic mills, baths, stirrers, and high-pressure homogenizers are used for the dispersion of nanoparticles. Baby and Sundara [59] used an economical method to synthesize hydrogen-functionalized, exfoliation-induced silver-decorated graphene (Ag/HEG) and prepared nanofluids. Ag/HEG was distributed in a mixture of deionized water/ethylene glycol using ultrasonic agitation without surfactant. The hybrid nanofluid was observed to be stable for more than 3 months. Aravind and Ramaprabhu [62] prepared MWCNT nanocomposites with graphene shells and synthesized them by chemical vapor deposition. The prepared hybrid nanofluid was stable for an extended period. Megatif et al. [80] prepared a CNT-TiO₂ hybrid nanocomposite and dispersed it in water to obtain a hybrid nanofluid. The surfactant SDBS was added to the suspension for proper dispersion. They sonicated the solution for 15 min and tested its stability. The solution was stable for 2 days.

Although most (95%) of the researchers adhered to the two-step method, nanofluids synthesized by the expensive and complex one-step method improve the stability of nanoparticle suspensions in base oils due to high sedimentation rates with short sonication times [108]. Ultrasonication lessens the sedimentation of nanoparticles, resulting in enhanced nanofluid stability. A better understanding of the mechanisms of nanofluids at the atomic level is required to address particle transport, aggregation, and stability issues with minimal experimentation.

No sophisticated equipment is required to produce nanofluids using a simple two-step method. Dispersion of nanoparticles requires sonication times of 3–10 h [109]. Amin et al. [110] critically reviewed the properties of single and hybrid nanofluids based on organic and synthetic materials. Malika and Sonavan [111] used a two-step method to prepare CuO–ZnO/water hybrid nanofluids. Ultrasonication provided nanofluid stability. FESEM/EDS, dynamic light scattering, and zeta potential measurements provide insight into nanoparticle morphology, shape, and size. The stability of Al₂O₃–CuO/(50/50) EG/W (ethylene glycol/water) hybrid nanofluids at 60 °C was confirmed by zeta potential measurements [112].

The stability of trihybrid nanofluids was tested by mixing three types of nanoparticles (i.e., Al₂O₃, TiO₂, and SiO₂ with volume concentrations of 0.05–0.3%) in a water/ethylene glycol-based fluid [113] and a recommended sonication time of 10 h at a zeta potential of 25.1 mV. To improve the stability of nanofluids, Afshari et al. [114] highlighted properties such as the acidity degree of the nanofluid, ultrasonication, nanoparticle material, base fluid type, nanoparticle concentration, surfactants, and surface modification of nanoparticles. Arora and Gupta [115] reviewed stability evaluation techniques (spectral absorbance, sedimentation, zeta-potential, and electron microscopy) and enhancement techniques (ultrasonication, surfactant addition, particle surface modifications, and pH change). Future research should focus on industrial applications to minimize pressure losses, the concentration of nanoparticles, and the long-term stability of hybrid nanofluids.

The stability characteristics of mono and hybrid nanofluids have been studied using zeta potential measurements and vibrating sample magnetometry (VSM) analysis [116]. To maintain nanofluid stability, Zainon and Azmi [29] recommend analysis by sonication, pH modification, surfactant, TEM, field emission scanning electron microscopy (FESEM), XRD, zeta potential, and UV/visible spectroscopy techniques. Bumataria et al. [117] used single and hybrid nanofluids to study heat transfer consider in heat pipe technologies. The use of dispersing agents and sonication increases the stability of nanofluids [118]. Excellent suspension stability could be obtained by adding small amounts of SDBS and PEG to DW (hybrid nanofluid 25% Al₂O₃ + 75% TiO₂) [119]. The hybrid nanofluid's stability was high, as the zeta potential value (i.e., the electrostatic repulsive force between the nanoparticle and the base fluid) was 42.6 mV compared to the reference value of 30 mV. Said et al. [120]

investigated the stability of carbon nanofibers (CNF), functionalized carbon nanofibers (F-CNF), reduced graphene oxide (rGO), and F-CNF/rGO nanofluids. Hybrid nanofluids (FCNF/rGO) showed higher stability than CNF, F-CNF, and rGO nanofluids.

Muthoka et al. [121] investigated the stability of hybrid nanofluids with two nanoparticles in PCM/DI water. The stability of surfactant-free MgO and 24 wt.% primary liquid was poor after 24 h, whereas the functionalized MWCNT solution showed no separation after 24 h. It was confirmed that the nanofluid's low-temperature stability was increased using a surfactant. Acid treatment with CNF was used to test stability [122]. The zeta potential of 0.02 vol.% F-CNF nanofluids measured after 2 and 90 days was -42.9 and -41.8 mV, indicating improved stability compared to the -16.3 and -15.5 mV UNV zeta potentials, which were characterized by relatively unstable dispersion. Alawi et al. [123] synthesized aqueous nanofluids PEG-GnP, PEG-TGr, Al_2O_3 , and SiO_2 . The dispersion stability of the carbon-based nanofluid and the metal oxide nanofluid was observed for 30 days, and the high dispersibility of PEG-HNP and PEG-TGr in an aqueous medium with low sedimentation was confirmed. Compared to GnP/DW nanofluids, TiO_2 /DW nanofluids showed superior stability [124]. The addition of CTAB surfactant showed excellent stability of ternary hybrid nanofluids [125]. Uysal [126] used a 500 rpm homogenizer to mix and stabilize nano-graphene in vegetable oil. Al-Waeli et al. [127] demonstrated high nanofluid stability (over 80 days) with CTAB and tannic acid + ammonia solution. The stability of Al_2O_3 /water nanofluids using CTAB and SDBS surfactants was investigated for various pH values [128]. Kazemi et al. [129] visually observed the stability of SiO_2 /water and G/water nanofluids. SiO_2 /water nanofluids were found stable at all pH values (see Table 2 for the stability of various nanofluids).

Table 2. Stability of different nanofluids with surfactants.

Author(s)	Nanoparticle	Base Fluid	Surfactant (s)
Xian et al. [130]	COOH-GnP, TiO_2	DW/EG	SDC, CTAB *, SDBS
Almanassra et al. [131]	CNT	Water	GA *, PVP, SDS
Cacua et al. [132]	Al_2O_3	Water	CTAB, SDBS *
Kazemi et al. [129]	SiO_2 , graphene	Water	CMC *
Ouikhalfan et al. [133]	TiO_2	DW	CTAB *, SDS
Siddiqui et al. [134]	Cu- Al_2O_3	DI water	
Cacua et al. [128]	Al_2O_3	DI water	CTAB, SDBS *
Etedali et al. [135]	SiO_2	DI water	CTAB *, SLS *
Giwa et al. [136]	Al_2O_3 - Fe_2O_3	DW	SDS *, NaDBS *
Kazemi et al. [137]	G- SiO_2	DW	CMC *
Gallego et al. [138]	Al_2O_3	Water	SDBS *
Shah et al. [139]	(rGO)	EG	CTAB *, SDBS, and SDS
Ilyas et al. [140]	GnP	Saline water	SDS *

* Recommended surfactant for improved stability of hybrid nanofluids.

Brownian motion of nanoparticles, micro-convection, clustering, and pH value strongly affect the thermal properties of hybrid nanofluids [141]. Solidification and clustering of nanocomposites of different sizes in nanofluids affect their thermal properties [142,143]. The stabilization and evaporation of single and hybrid nanofluids have been studied in specific systems from a statistical point of view [144,145].

4. Thermo-Physical Properties of Mono/Hybrid Nanofluids

This section summarizes the influence of using hybrid nanofluids on effective thermal conductivity, dynamic viscosity, density, and specific heat [146–148]. Devices commonly used for measuring the properties (density, specific heat, thermal conductivity, and viscosity) of working fluids, including nanofluids and hybrid nanofluids, are shown in Figure 4. The density of a liquid can be measured by taking the weight of the liquid and dividing it by its volume. A digital scale can be used to measure mass. Viscosity can be measured with a Brookfield DV1 digital viscometer, and thermal conductivity and specific heat can be measured with a hot disc thermal constant analyzer.



Figure 4. Photographs of (a) digital weighing balance, (b) Brookfield DV1 digital viscometer, and (c) hot disc thermal constant analyzer apparatus [48].

4.1. Density and Specific Heat of Mono/Hybrid Nanofluids

Density and specific heat capacity are among the most important thermo-physical properties of hybrid nanofluids when studying the heat transfer properties of working fluids. Ho et al. [149] studied aqueous hybrid nanofluids of Al_2O_3 nanoparticles and microencapsulated particles of phase change materials. They measured various thermo-physical properties of the hybrid nanofluids. Baghbanzadeh et al. [150] studied the thermo-physical properties of aqueous hybrid nanofluids containing different weights of silica and MWCNTs. They observed that the density and viscosity of the hybrid nanofluids increased with concentration but decreased with increasing temperature. Labib et al. [151] found that density increased more than the viscosity with the volume fraction of a hybrid suspension containing carbon nanotubes and oxides.

Some studies of hybrid nanofluids concluded that the specific heat increases with particle volume concentration and temperature, while the density enhances with concentration and drops with the temperature. The increase in specific heat is related to the formation of nanostructures at the solid–liquid interface, whereas particle aggregation harms the increase in specific heat. The hybrid nanofluid’s density ratio [152] is obtained from the mass balance and the specific heat capacity from the energy balance. The generalized form of the density and specific heat equations for hybrid nanofluids are as follows:

$$\rho_{nf} = \sum \phi_p \rho_p + \rho_{bf}(1 - \sum \phi_p), \quad (1)$$

$$\rho_{nf} c_{nf} = \sum \phi_p \rho_p c_p + \rho_{bf} c_{bf}(1 - \sum \phi_p), \quad (2)$$

where ρ is the density, ϕ is the volume fraction, and c is the specific heat.

4.2. Viscosity of Mono/Hybrid Nanofluids

Viscosity is one of the critical thermophysical properties for studying the behavior of hybrid nanofluids because the required pressure drop and pump operation depend on it. Numerous physical parameters affect the viscosity of nanofluids. Large particles

have a relatively higher viscosity than small particles [153]. Nanofluids at low volume concentrations exhibit Newtonian behavior [154]. Ho et al. [149] reported the viscosity of a 10 wt.% hybrid suspension compared to water. Baghbanzadeh et al. [150] studied the rheological properties of aqueous hybrid nanofluids containing silicon dioxide and MWCNTs in weight ratios of 80:20 and 50:50. They observed that the nanofluid's viscosity increased as the concentration and temperature decreased. The viscosity increase was the smallest for the 50:50 wt.% ratio. Abashi et al. [65] measured the viscosity of MWNT–TiO₂/water suspensions. They observed an increase in fluid viscosity, and the enhancement was more significant when there were more MWCNT nanoparticles than TiO₂ nanoparticles in the solution. Sundar et al. [68] experimentally determined the viscosity of the nanocomposite hybrid nanofluid MWCNT–Fe₃O₄ and observed an increase in viscosity up to 1.5 times at 3 vol.% concentration and 60 °C compared to water.

Esfe et al. [155] and Dardan et al. [156] studied an oil-based hybrid nanofluid containing MWCNT nanoparticles. They observed a significant increase in viscosity. Soltani and Akbari [157] studied ethylene glycol-based hybrid nanofluids containing MgO and MWCNT nanoparticles. They observed an increase in viscosity of up to 168% when increasing the particle volume fraction to 1.0%. Esfe et al. [158] studied the viscosity of MWCNT–TiO₂ hybrid nanofluids using brine as the base fluid. They observed an 83% increase in viscosity at 10 °C. Asadi and Asadi [159] proposed a correlation for the viscosity of motor oil-based hybrid nanofluids containing MWCNTs and ZnO nanoparticles (15:85). The maximum increase in viscosity was about 45% at 55 °C and 1.0% concentration. Suresh et al. [56] tested a hybrid nanofluid of aluminum oxide and copper, showing that the viscosity increased by 115% at a concentration of 2.0 vol.%. At low concentrations, the effect was negligible. Suspensions containing silica and silver particles had lower viscosities than those containing only silica particles [57]. A 24% increase in viscosity was observed at a concentration of 0.02 vol.% [160].

Yarmand et al. [161] found a 30% increase in viscosity and 0.09% density for the nanocomposite hybrid nanofluid GNP–silver at 40 °C. The thermal conductivity and viscosity of nanodiamond–Fe₃O₄ nanofluids were noted for 20 to 60 °C temperature and concentrations up to 0.2 vol.% [162]. They suggested a correlation for the viscosity ratio at different temperatures, which was exponential and depended only on the volume concentration. An expression was proposed for the viscosity of hybrid oil-based MWCNT nanofluids at 25–60 °C [155,163,164]. A correlation for the viscosity of the hybrid nanofluids was established according to the shape function [165].

$$\frac{\mu_{nf}}{\mu_{bf}} = 1 + \psi_1\phi + \psi_2\phi^2, \quad (3)$$

where ϕ is the total volume fraction of particles. μ_{nf} and μ_{bf} are the viscosities of the hybrid nanofluid and base fluid, respectively, and Ψ_1 and Ψ_2 are coefficients, whose values were given by Sheikholeslami and Shamlooei [165]. Correlations for the viscosity and viscosity ratio for different hybrid nanofluids are summarized in Table 3. The viscosity data obtained from the test and proposed empirical relations were compared for the 0.1% volume concentration of alumina nanofluid (Figure 5). It can be observed that some results matched the test data, whereas others showed deviation. The reason can be negligence of particle size or working temperature, whereas different relationships may be valid for other working parameters. Therefore, researchers must choose an appropriate empirical ratio or develop one suitable for the nanofluid synthesized.

Table 3. Summary of correlation for the viscosity of hybrid nanofluids.

Author(s)	Nanoparticle/Base Fluid	Working Condition	Correlation
Esfe et al. [160]	Ag–MgO (50: 50)/water	$\phi = 0\text{--}2\%$	$\frac{\mu_{nf}}{\mu_{bf}} = 1 + 32.795\phi - 7214\phi^2 + 714600\phi^3 - 0.1941 \times 10^8\phi^4$

Table 3. Cont.

Author(s)	Nanoparticle/Base Fluid	Working Condition	Correlation
Asadi and Asadi [159]	MWCNT–ZnO (15:85)/engine oil	T = 5–55 °C, $\phi = 0.125$ –1.0%	$\mu_{nf} = 796.8 + 76.26\phi + 12.88T + 0.7965\phi T - 196.9\sqrt{T} - 16.53\phi\sqrt{T}$
Afrand et al. [163]	MWCNT–SiO ₂ (equal portion)/SAE40	T = 25–60 °C, $\phi = 0$ –1%	$\frac{\mu_{nf}}{\mu_{bf}} = 0.00337 + \exp(0.07731\phi^{1.452}T^{0.3387})$
Asadi et al. [166]	MWCNT–MgO (20:80)/SAE50	T = 25–50 °C, $\phi = 0$ –2%	$\frac{\mu_{nf}}{\mu_{bf}} = (328201T^{-2.053}\phi^{0.09359})$
Dardan et al. [156]	MWCNT–Al ₂ O ₃ (25:75)/SAE40	T = 25–50 °C, $\phi = 0$ –2%	$\frac{\mu_{nf}}{\mu_{bf}} = 1.123 + 0.3251\phi - 0.08994T + 0.002552T^2 - 0.00002386T^3 + 0.9695\left(\frac{T}{\phi}\right)^{0.01719}$
Soltani and Akbari [157]	MWCNT–MgO/EG	T = 30–60 °C, $\phi = 0.1$ –1.0%	$\frac{\mu_{nf}}{\mu_{bf}} = [0.191\phi + 0.240(T^{-0.342}\phi^{-0.473})] \times \exp(1.45T^{0.120}\phi^{0.158})$

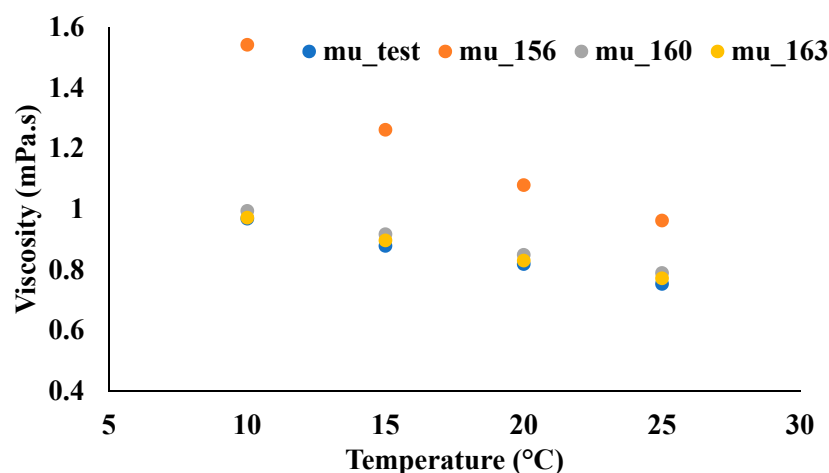


Figure 5. Comparison of experimental and empirical results for viscosity.

4.3. Thermal Conductivity of Mono/Hybrid Nanofluids

Thermal conductivity is one of the essential physical properties of fluid for improving the heat transfer performance of a working fluid because the heat transfer characteristics increase as the thermal conductivity increases. The mechanism of Brownian motion enhances the thermal conductivity of nanofluids at low temperatures [167]. Hamze et al. [168] studied the influence of thermal conductivity on FLG properties. Triton X-100 surfactant increased thermal conductivity and dynamic viscosity in [169]. Batmunkh et al. [70] showed a 0.8% increase in thermal conductivity for silver–titanium hybrid nanofluids. Hybrid silver–magnesium nanofluids showed a rise of 8.6% in thermal conductivity at a concentration of 0.02 vol.% [160]. Charab et al. [170] developed a thermal conductivity model for Al₂O₃–TiO₂ hybrid nanofluids. They found a nonlinear relationship between particle volume concentration and thermal conductivity due to stability issues in nanofluids.

Baghbanzadeh et al. [150] observed 23.3% and 8.8% increases in thermal conductivity for MWCNT nanofluids and silica nanofluids. The effect of nanoparticle shape on fluid thermal conductivity was examined using alumina–MWCNT hybrid nanofluids [171]. The thermal conductivity was found to be enhanced. However, spherical particles give better results than cylindrical particles. Sundar et al. [68] and Shahsavari et al. [172] saw increased thermal conductivity when using CNT–Fe₃O₄ hybrid nanofluids. Farbod and Ahangarpour [173] and Munkhbayar et al. [67] studied the thermal properties of water-based hybrid Ag–MWCNT nanofluids. They found that the resulting thermal conductivity was 20% and 14.5% higher than the base fluid. Soltani and Akbari [157] analyzed ethylene glycol-based hybrid nanofluids containing MgO and MWCNT nanoparticles. Thermal conductivity increased by 14.5% at 40 °C. Harandi et al. [174] experimentally studied the

thermal conductivity of EG-based hybrid nanofluids containing functionalized MWCNTs and Fe₃O₄ nanoparticles. They found an augmentation in thermal conductivity of 30% at a temperature of 50 °C and a concentration of 2.3%.

Botha et al. [57] studied an oil-based hybrid nanofluid of silver and silica (a nano lubricant) and observed a 15% increase in thermal conductivity for 0.6 wt.% Ag and 0.7 wt.% silica by weight. Al₂O₃–Cu hybrid nanofluids gave better results than aluminum oxide nanofluids with an augmented thermal conductivity of 12.11% [56]. Adding 0.2 vol.% ND–Fe₃O₄ nanoparticles increased the thermal conductivity of water by 17.8% [162]. Yarmand et al. [175] studied the thermal conductivity of graphene (0.06 wt.%) activated a carbon suspension in ethylene glycol and observed 4.17% and 6.47% increases at 20 °C and 40 °C. Various researchers have proposed correlations for hybrid nanofluids with various base fluids (deionized water, motor oil, vegetable oil, glycols, mixtures of glycols, and water). Table 4 summarizes the correlations proposed by the researchers for the thermal conductivity of hybrid nanofluids.

Table 4. Summary of correlation for the thermal conductivity of hybrid nanofluids.

Author(s)	Nanoparticle/Base Fluid	Working Condition	Correlation
Chougule and Sahu [176]	-	-	$\frac{k_{eff}}{k_{bf}} = 1 + \frac{k_{p1}\phi_1\tau_{bf}}{k_{bf}\tau_{p1}(1-\{\phi_1+\phi_2\})} + \frac{k_{p2}\phi_2\tau_{bf}}{k_{bf}\tau_{p2}(1-\{\phi_1+\phi_2\})}$
Takabi and Salehi [177]	Al ₂ O ₃ –Cu/water	$\phi = 0.1\text{--}2.0\%$	$\frac{k_{nf}}{k_{bf}} = \frac{\phi_1k_1+\phi_2k_2}{\phi} + 2(1-\phi)k_{bf} + 2(\phi_1k_1+\phi_2k_2)$ $\frac{k_{nf}}{k_{bf}} = \frac{\phi_1k_1+\phi_2k_2}{\phi} + (2+\phi)k_{bf} - (\phi_1k_1+\phi_2k_2)$
Esfe et al. [178]	CNTs–Al ₂ O ₃ /water	T = 27–57 °C, $\phi = 0\text{--}1\%$	$\frac{k_{nf}}{k_{bf}} = 1.05 + 0.005T + 0.06\phi + 0.0099\phi T + 0.00317T^2 + 0.026\phi^2 + 0.0034T^2\phi + 0.00735T\phi^2$
Esfe et al. [160]	Ag–MgO (equal)/water	$\phi = 0\text{--}2\%$	$\frac{k_{nf}}{k_{bf}} = \frac{0.1747 \times 10^5 + \phi}{0.1747 \times 10^5 - 0.1498 \times 10^6 \phi + 0.1117 \times 10^7 \phi^2 + 0.1997 \times 10^8 \phi^3}$
Esfe et al. [179]	Cu–TiO ₂ /water–EG (60:40)	T = 30–60 °C, $\phi = 0.1\text{--}2.0\%$	$\frac{k_{nf}}{k_{bf}} = 1.07 + 0.000589T - \frac{0.000184}{\phi T} + 4.44T\phi \times \cos(6.11 + 0.00673T + 4.41\phi T - 0.0414\sin T) - 32.5\phi$
Esfe et al. [180]	DWCNT–ZnO/water–EG (60:40)	T = 25–50 °C, $\phi = 0.025\text{--}1.0\%$	$\frac{k_{nf}}{k_{bf}} = 0.0288 \times \ln(\phi) + 1.085 \exp(0.001351T + 0.13\phi^2)$
Harandi et al. [174]	MWCNT–Fe ₃ O ₄ (equal)/EG	T = 25–50 °C, $\phi = 0.1\text{--}2.3\%$	$\frac{k_{nf}}{k_{bf}} = 1 + 0.0162\phi^{0.7038}T^{0.6009}$
Afrand [181]	MgO–fMWCNT/EG	T = 25–50 °C, $\phi = 0.0\text{--}0.6\%$	$\frac{k_{nf}}{k_{bf}} = 0.8341 + 1.1\phi^{0.243}T^{-0.289}$
Vafaei et al. [182]	MgO–MWCNT/EG	T = 25–50 °C, $\phi = 0.0\text{--}0.6\%$	$\frac{k_{nf}}{k_{bf}} = 0.9787 + \exp(0.3081\phi^{0.3097} - 0.002T)$
Esfe et al. [183]	SWCNT–MgO (20:80)/EG	T = 30–50 °C, $\phi = 0.0\text{--}2.0\%$	$\frac{k_{nf}}{k_{bf}} = 0.90844 - 0.06613\phi^{0.3}T^{0.7} + 0.01266\phi^{0.31}T$
Esfe et al. [184]	MWCNT–SiO ₂ (15:85)/EG	T = 30–50 °C, $\phi = 0.0\text{--}2.0\%$	$\frac{k_{nf}}{k_{bf}} = 0.905 + 0.002069T\phi + 0.04375\phi^{0.09265}T^{0.3305} - 0.0063\phi^3$
Esfe et al. [185]	MWCNT–SiO ₂ (30:70)/EG	T = 30–60 °C, $\phi = 0.025\text{--}0.86\%$	$\frac{k_{nf}}{k_{bf}} = 1.01 + 0.007685T\phi - 0.5136\phi^2T^{-0.1578} + 11.5\phi^3T^{-1.175}$
Esfe et al. [186]	DWCNT–SiO ₂ /EG	T = 30–50 °C, $\phi = 0.03\text{--}1.71\%$	$\frac{k_{nf}}{k_{bf}} = 0.9896 - 0.07122\phi + (0.02705\phi^{0.7685}T^{0.627}) + 1.531 \times 10^{-5}T^2$
Esfe et al. [187]	SWCNT–Al ₂ O ₃ (15:85)/EG	T = 30–50 °C, $\phi = 0.0\text{--}2.5\%$	$\frac{k_{nf}}{k_{bf}} = 0.963 + 0.008379[\phi^{0.4439} \times T^{0.9246}]$
Rostamian et al. [188]	CuO–SWCNT (50:50)/water–EG (60:40)	T = 20–50 °C, $\phi = 0.02\text{--}0.75\%$	$\frac{k_{nf}}{k_{bf}} = 1 + 0.04056\phi T - 0.003252(\phi T)^2 + 0.0001181(\phi T)^3 - 0.000001431(\phi T)^4$
Zadkhash et al. [189]	MWCNT–CuO/water	T = 25–50 °C, $\phi = 0.0\text{--}0.6\%$	$\frac{k_{nf}}{k_{bf}} = 0.907\exp(0.36\phi^{0.3111} + 0.000956T)$

Elias et al. [190] proposed the following correlation for the thermal conductivity of hybrid nanofluids according to their shape function:

$$\frac{k_{nf}}{k_{bf}} = \left(\frac{k_1 + (n_1 - 1)k_{bf} - (n_1 - 1)(k_{bf} - k_1)\phi_1}{k_1 + (n_1 - 1)k_{bf} + (k_{bf} - k_1)\phi_1} \right) \left(\frac{k_2 + (n_2 - 1)k_{nf} - (n_2 - 1)(k_{nf} - k_2)\phi_2}{k_2 + (n_2 - 1)k_{nf} + (k_{nf} - k_2)\phi_2} \right), \quad (4)$$

where n_1 and n_2 are shape functions whose values differ for different shapes. k_{nf} and k_{bf} are the thermal conductivities of the hybrid nanofluid and base fluid, respectively. k_1 and k_2 are the thermal conductivities of particles 1 and 2, respectively. ϕ_1 and ϕ_2 are the volume fractions of particles 1 and 2, respectively. Different shapes, such as cylinders, blades, bricks, and plates, were considered in [190], revealing that cylindrical particles performed better than other shapes.

For thermal conductivity, some empirical relationships have been presented that are not valid for all nanofluids with different concentrations of nanoparticles. This can be seen from Figure 6, where test data are compared with the results obtained from other empirical relations. Therefore, researchers must choose an appropriate empirical ratio or develop a relation suitable for the developed nanofluid. It was observed that the viscosity and thermal conductivity of the working fluid increased with the addition of nanoparticles. The researchers observed this at low concentrations of nanoparticles and assumed that the same trend would continue at higher concentrations. Experiments revealed that the Prandtl number (ratio of viscosity to thermal conductivity) increases up to a specific concentration of nanoparticles. Then, it starts to fall because the two properties do not increase proportionally [190]. This increasing–decreasing trend in the Prandtl number affects the Nusselt number, which in turn affects the performance of the heat exchanger.

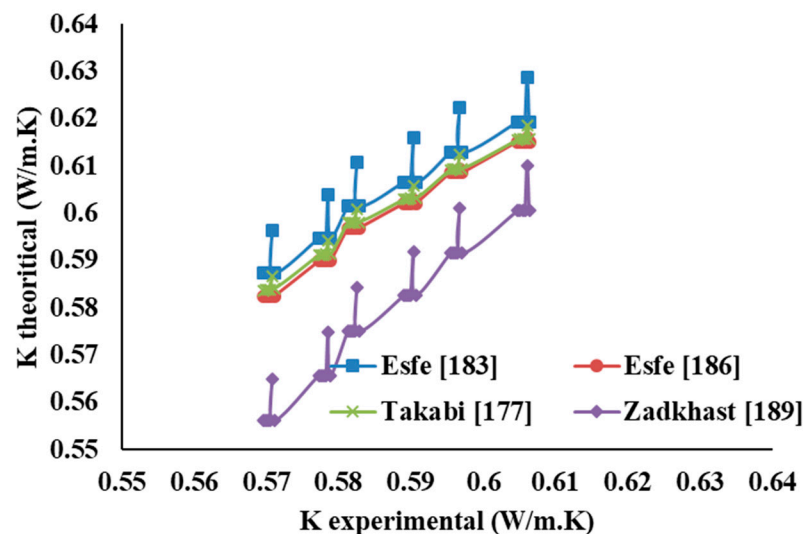


Figure 6. Comparison of experimental and empirical results for thermal conductivity.

Table 5 represents the thermo-physical properties of different fluids measured by devices mentioned in Figure 4. It also shows the variation of properties at different working temperatures (10–25 °C). It can be observed that the thermal conductivity, density, and viscosity increase with the addition of nanoparticles in the base fluid. The fluid's thermal conductivity increases with the temperature increase, whereas density and viscosity decrease. No change is observed for the specific heat as the studied temperature range is small. Table 6 compares the test data and theoretical data obtained from Equations (1)–(4) for different thermo-physical properties of alumina nanofluid with 0.1 vol.% concentration. It can be observed that the specific heat and density data are the same for the experimental data and theoretical prediction from the empirical relation. Whereas there is a deviation in the case of thermal conductivity and viscosity, as indicated in the provided empirical relations, the influence of temperature and particle size is neglected. Hence, correlations containing the effect of temperature and particle size are needed for predicting accurate results.

Table 5. Experimental data for thermo-physical properties of different fluids.

T (°C)	Water	TiO ₂ (0.1 vol.%)	Al ₂ O ₃ (0.1 vol.%)
Thermal conductivity, k (W/m-K)			
10	0.5823	0.5919	0.5922
15	0.5896	0.5979	0.5994
20	0.5964	0.6036	0.6047
25	0.6014	0.6091	0.6109
Density, ρ (kg/m ³)			
10	997.8	1001.0	1000.7
15	996.8	1000.0	999.5
20	996.0	999.0	998.6
25	994.7	997.9	997.3
Viscosity, μ (mPa·S)			
10	0.9549	0.9684	0.9684
15	0.8706	0.8935	0.8786
20	0.8150	0.8275	0.8187
25	0.7493	0.7690	0.7535
Specific Heat, C_p (J/kg·K)			
10	4183	4168	4170
15	4183	4169	4169
20	4183	4169	4169
25	4183	4169	4169

Table 6. Comparison of experimental and theoretical data for thermo-physical properties of Al₂O₃ nanofluid.

T (°C)	K_Test (W/m-K)	K_th (W/m-K)	μ_{test} (mPa·S)	μ_{th} (mPa·S)	C_{p_test} (J/kg·K)	C_{p_th} (J/kg·K)	ρ_{test} (kg/m ³)	ρ_{th} (kg/m ³)
10	0.5922	0.5829	0.9684	0.9559	4170	4170	1000.7	1001
15	0.5994	0.5902	0.8786	0.8715	4169	4169	999.5	1000
20	0.6047	0.597	0.8187	0.8158	4169	4169	998.6	999
25	0.6109	0.602	0.7535	0.7501	4169	4169	997.3	997.7

5. Hydrothermal Characteristics of Heat Exchanger

Focused extensive research is being conducted to enhance the performance of heat exchangers under laminar and turbulent flow. Providing the corrugation and chevron angle on a flat surface augments the heat transfer behavior because it increases the surface area and includes turbulence, further increasing the heat transfer coefficient [191]. Different mono and hybrid nanofluids have been introduced to enhance the performance of thermal devices, and their hydrothermal characteristics have been studied [192–202]. Heat transfer increases with the heat transfer coefficient, which nanofluids enhance due to increased thermal conductivity via several mechanisms. It was observed that heat transfer and pressure drop both increase using nanofluids, but the rise in pressure drop is comparatively insignificant. This section is divided into two parts: experimental and numerical studies of mono/hybrid nanofluids for heat exchangers (plate heat exchanger, tubular heat exchanger, mini-channel heat exchanger, and heat pipe).

5.1. Experimental Studies on Heat Exchangers

Pandey and Nema [203] analyzed an alumina–water solution as the refrigerant in a corrugated plate heat exchanger. They observed enhanced heat transfer properties with the Reynolds number. Tiwari et al. [204,205] conducted experimental studies on plate heat exchangers using various nanofluids to improve their performance. Barzegarian et al. [206] studied the hydrothermal characteristics of a plate heat exchanger for domestic hot water application using TiO₂–water nanofluid. Tabari et al. [207] used TiO₂–water nanofluid in a PHE for milk pasteurization considering mass concentrations (0.25%, 0.35%, and 0.8%) and concluded that the heat transfer rate increased due to the increased thermal conductivity. The effect of plate orientation in an alumina nanofluid plate heat exchanger was studied experimentally by Prashant et al. [208]. They found that the heat transfer decreased with the Reynolds number when the plate orientation was changed from horizontal to vertical. The heat transfer coefficient was reduced by 10–15% at a tilt angle of 30°. Huang et al. [209] used a mixture of Al₂O₃–water and MWCNT–water at a ratio of 2.5:1 in a plate heat exchanger and observed an increase in HTC and a pressure drop when using the hybrid solution compared to the primary fluid. Bhattad et al. [210,211] conducted experiments with plate heat exchangers using different hybrid nanofluids as refrigerants and observed changes in the volume ratio of the particles and an influence of particle size on the heat exchanger performance. They discussed the ranking of different fluids based on the achieved thermal conductivity, viscosity, density, and specific heat properties. According to heat transfer performance, studied nanofluids were arranged in ascending order as TiO₂, CuO, Al₂O₃, MgO, AlN, SiC, and MWCNT. Similarly, according to pump work, different fluids were arranged in descending order as MWCNT, CuO, TiO₂, Al₂O₃, MgO, AlN, and SiC. Bhattad [212,213] performed experiments with hybrid nanofluids in plate heat exchangers and found that hybrid nanofluids increased the heat transfer efficiency of the heat exchanger.

Kavitha et al. [214] experimented with CuO–water nanofluid as a coolant to improve a two-tube heat exchanger. Jassim and Ahmed [215,216] experimentally evaluated the effect of Al₂O₃ nanofluids on heat exchanger performance. Mansoury et al. [217] experimentally studied the heat transfer characteristics and flow of Al₂O₃–water nanofluids in heat exchangers. Pipe heat exchangers offer higher heat transfer coefficients than plate heat exchangers. Henein et al. [218] improved the thermal performance of a heat pipe vacuum tube solar collector using MgO–MWCNT/water hybrid nanofluids as the working fluid. It was interpreted that the energy and exergy efficiency increased as the mass ratio of MWCNT nanoparticles increased. The heat transfer properties of heat exchangers were improved [219–223]. Cylindrical (MWCNT) and various spherical (MgO) nanoparticles have been used to study the properties of two-pipe heat exchangers [224,225]. The heat transfer rate was increased by 115% using the MWCNT nanofluid. Subramanian et al. [226] experimentally found that the heat transfer of the TiO₂–water nanofluid was higher than that of the primary fluid (water). The pump work required due to the differential pressure could be estimated from the equations mentioned in the study by Dalkilic et al. [227]. Bahmani et al. [228] studied forced convection in a tube heat exchanger using a nanofluid (aluminum oxide/water). The extreme increase rate of the average Nusselt number and increase rate of thermal efficiency were 32.70% and 30%, respectively. Later, Bahmani et al. [229] studied forced convection in a two-tube heat exchanger with nanofluids at various Reynolds numbers ranging from 100 to 1500. Kristiawan et al. [230] observed enhancement in the thermal performance of helical micro-fin tubes using titania nanofluid with different particle concentrations. They also proposed a correlation to predict the Nusselt number.

Heat pipes are designed to act as heat transfer and thermostats. They were first introduced by Akachi [231]. A survey was conducted on heat pipe stability and operating limitations [232]. The heat transfer ability of nanofluid-filled PHP depends more on factors such as the nanofluid's thermal conductivity and viscosity. A variety of nanoparticles, including metals [233], oxide particles [234], graphene, graphene oxide [235], and

diamond particles [236], have been tested to understand their effect on the heat transfer properties of a PHP. Heat flux increases with nanofluid concentration, while a higher concentration leads to a higher viscosity [237]. Qu and Wu [238] tested the thermal performance of a PHP using SiO₂/water and Al₂O₃/water nanofluids. Experimental results showed that the Al₂O₃/water nanofluid improved the heat transfer performance of the PHP. Goshayeshi et al. [239] compared the properties of CLPHP charged with nanofluid Fe₃O₄ and γ-Fe₂O₃. Results showed that Fe₃O₄ exhibits higher thermal performance than γ-Fe₂O₃.

The thermal resistance and critical thermal load of FP-PHP decreased with increasing nanoparticle concentration/mass fraction [240]. Li [235] investigated the change in heat transfer efficiency in a PHP of graphene/water–ethylene glycol nanosuspensions at various concentrations and packing factors. Xu et al. [241] performed experiments considering hybrid working fluids. Zufar et al. [242] investigated a PHP using various hybrid nanofluids and concluded that the thermal resistance of the PHP for SiO₂–CuO and Al₂O₃–CuO hybrid nanofluids was 50% and 34% lower than that of water, respectively. Khodami et al. [243] studied a PHP heat exchanger prototype. The results showed that silver nanofluid improved exergy efficiency and reduces exergy loss. Jahani et al. [244] studied the thermal properties of nanofluidic PHP charges. The results showed the improvement in PHP performance using silver nanofluid. Su et al. [245] showed that self-wetting nanofluids have better heat transfer properties than charged self-wetting liquids and nanofluids alone over the entire operating range.

Several experimental studies on the hydrothermal behavior of HyNfs in mini/micro-channel heat sinks are available [246]. Selvakumar and Suresh [247] synthesized hybrid AlO–Cu nanoparticles and studied the properties of HyNf Al₂O₃–Cu/water in a mini-channel. Ahammed et al. [248] showed a 63.13% increase in the convective heat transfer coefficient when using HyNf Al₂O₃–graphene in a mini-channel. Nimmagadda and Venkatasubbaiah [249] experimentally studied the behavior of Al₂O₃–Ag HyNf in microchannels. Ho et al. [250] looked at nano-encapsulated phase change materials at MCHS and found up to 70% improvement in heat transfer. Kumar and Sarkar [251] determined various combinations of HyNf-based nanoparticles in MCHS and showed that the Al₂O₃–AlN combination performed best. Similar investigations on micro/mini-channel heat exchange devices using HyNfs were performed in [252–259].

5.2. Numerical Studies on the Heat Exchangers

Pantzali et al. [260] investigated the operation of a miniature plate heat exchanger whose surface was modulated using nanofluids. It has been reported that using the nanofluid of CuO/water reduces the equipment's size and the pump's operation. Gherasim et al. [261] studied the heat transfer and flow properties of plate-like HEX using a homogeneous model with CuO and aluminum oxide nanofluids. They found that the heat transfer rate increased at higher pressure drops using nanofluids. The performance of various nanofluids (1.0 vol.%) in a small plate heat exchanger was examined [262]. They found the need for an increase in the convective heat transfer coefficient, as well as decreases in the volumetric flow rate and pumping power. A single-phase numerical model obtained promising results with various nanofluids [263]. Stogiannis et al. [264] numerically observed decreases in coolant consumption and pumping power with SiO₂ nanofluid coolant in a PFC. In the course of numerical studies conducted by Jokar and O'Halloran [265], a clear conclusion was drawn regarding augmented thermal conductivity and a drop in heat transfer with increasing volumetric concentration. Goodarzi et al. [266] and Bhattad et al. [267] numerically studied MWCNT hybrid nanofluids on HEX plates in the turbulent regime. They noted that the heat transfer rate and pump work both increased.

Ding et al. [268] performed a numerical study of TiO₂/water nanofluids in a two-tube heat exchanger. The results showed that the nanofluid's heat transfer capacity was higher than that of deionized water. Bhattad and Babu [269] performed thermal evaluations of shell-and-tube heat exchangers using various alumina/water hybrid nanofluids. They found a 16.5% heat transfer rate gain using MWCNT/alumina hybrid nanofluid.

Jafarmadar et al. [270] investigated PHP's entropy generation and thermal analysis using Al_2O_3 , CuO, and Ag nanofluids. An optimal concentration of 0.5–1% of the nanoparticle volume was determined on the basis of mathematical modeling. Yan et al. [271] and Khetib et al. [272] performed a numerical study to determine the effect of different types of nanofluids on MCHS. Kalteh et al. [273] conducted a numerical study of forced convection heat exchange between alumina and copper nanofluids at MCHS. At a volume fraction of 0.03, the average Nusselt number of copper nanofluids increased by 29.41%.

Some of the relevant studies with significant results are listed in Table 7. The literature survey in the present section showed that the Nusselt number plays a very significant role in convective studies of fluid flow problems. Hence, the quantitative data for the Nusselt number are presented in Table 8.

Table 7. Summary of studies on HEX with mono and hybrid nanofluids.

Author(s)	Operating Variables	Nanofluid Characteristics	Findings
Pantzali et al. [274]	Nanofluid as coolant, PHE, $T_{ci} = 30$, $T_{hi} = 50$ °C, $\Omega_h = 40$ –56 mL/s, $\Omega_c = 10$ –100 mL/s	Al_2O_3 , CNT, TiO_2 , CuO/water (0.5–4.0 vol.%), surfactant: CTAB	The use of nanofluids was advantageous in laminar flow.
Zamzamian et al. [275]	Hot side: nanofluid, PHE, cold side: water, Ω_h : 3 lpm, Ω_c : 2.5 lpm, $T_{hi} = 45$ –75 °C	Al_2O_3 , CuO/EG (0.1–1.0 wt.%), surfactant: SDS, SDBS, and CTAB	HTC increased with increasing concentration and temperature by 3% to 49%.
Kabeel et al. [276]	Hot side: nanofluid, PHE, cold side: water, laminar flow, $T_{hi} = 40$ °C, $\Omega_c = 3$ m ³ /h	Al_2O_3 /water (1–4 vol.%)	HTC and pump work increased with ϕ . For 4.0 vol.%, HTC increased by 13%.
Tiwari et al. [277]	Nanofluid as coolant, PHE, $\Omega_h = 3$ lpm, $\Omega_c = 1.0$ –4.0 lpm, $T_{ci} = (25$ –50 °C), $T_{hi} = 70$ °C	CeO_2 /water (0.5–3.0 vol.%)	HTC increased by 39% at 0.75 vol.% with almost no pressure drop.
Khairul et al. [278]	PHE, nanofluid as coolant, $\Omega_c = 2$ –5 lpm, $\Omega_h = 2$ lpm, $T_{ci} = 300$ K	CuO/water (0.5–1.5 vol.%)	HTC increased by 27.20%, while exergy loss was reduced by 24% at 1.5 vol.%.
Huang et al. [279]	Hot side: nanofluid, PHE, cold side: water, counter flow, $\text{Re} = 58$ –624, $\Omega = 0$ –0.16 lps, $T_{hi} = 33$ °C, $T_{ci} = 22$ °C	Al_2O_3 /water (0.56–2.84 vol.%) and MWCNT/water (0.0111–0.0555 vol.%)	HTC and the pressure drop increased with concentration.
Tabari and Heris [280]	PHE, hot side: nanofluid, cold side: milk, counter flow, $\text{Pe} = 300$ –1100, $T_{hi} = 68$ –72 °C	MWCNT/water (0.25–0.55 wt.%)	HTC and heat transfer rates increased upon adding MWCNTs to the base fluid.
Abed et al. [281]	PHE, height = 2.5–5 mm, pitch = 6–12 mm, constant heat flux: 6 kW/m ² , $T_i = 300$ K, turbulent flow	Al_2O_3 , CuO, SiO_2 , and ZnO/water (0–4 vol.%)	The most desirable channel parameters were a trapezoid height of 5 mm and a vertical pitch of 6 mm.
Behrangzade and Heyhat [282]	PHE, hot side: nanofluid, cold side: water, $\Omega_c = 2$ –4 lpm, $\Omega_h = 4$ –8 lpm, $T_{hi} = 30$ –55 °C	Ag/water (100 ppm)	Overall, HTC increased by 16.79% for 100 ppm nanofluid.
Sarafraz and Hormozi [283]	PHE, $\text{Re}_h = 700$ –25000, $T_{hi} = 50$ –70 °C	MWCNT/water nanofluid (0.5–1.5 vol.%)	HTC increased with flow rate and volume concentration.
Sun et al. [284]	PHE, $\text{Re} = 1000$ –2800	(Cu, Fe_2O_3 , and Al_2O_3)/DI water (0.1–0.5%)	Overall, HTC increased with mass fraction of particles.
Kumar et al. [285]	PHE, $T_{ci} = 20$ °C, $T_{hi} = 50$ °C, $\Omega_c = 0.5$ –2 lpm, $\Omega_h = 3$ lpm, $\beta = 30^\circ/30^\circ$, $30^\circ/60^\circ$, $60^\circ/60^\circ$	ZnO/water (0–2 vol.%), surfactant: CTAB	The optimum increase in HTRR and HTCR, as well as reduction in exergy loss, was observed at 1.0 vol.% for β -60°/60°.
Kumar et al. [286]	PHE, Nanofluid as coolant, $T_{ci} = 20$ °C, $T_{hi} = 50$ °C, $\Omega_c = \Omega_h = 3$ lpm, $b = 2.5$ –10.0 mm	TiO_2 , Al_2O_3 , ZnO, CeO_2 , GNP, MWCNT nanofluids, Cu + Al_2O_3 hybrid nanofluid/DI water (0.5–2.0 vol.%), surfactant: CTAB	Exergy destruction was lowest and exergetic efficiency was maximum for 5 mm spacing at 0.75 vol.%.
Ahmed et al. [287]	Microchannel, $\text{Re} = 50$ –300, laminar flow	Al_2O_3 and SiO_2 /water (0.3–0.9 vol.%)	Al_2O_3 had the lowest thermal resistance. SiO_2 was preferred due to lower pressure drop.

Table 7. Cont.

Author(s)	Operating Variables	Nanofluid Characteristics	Findings
Ardeh et al. [288]	Microchannel, Re = 50–400, laminar flow	Al ₂ O ₃ –SiO ₂ , Al ₂ O ₃ –Cu/water (0–5 vol.%)	Al ₂ O ₃ –SiO ₂ hybrid nanofluid had a lower thermal resistance and better thermal performance.
Wang et al. [289]	Microchannel, Re = 340–640, laminar flow	Al ₂ O ₃ /water (1–4 vol.%), D = 20–40 nm	Nanoparticles with small diameters and high concentrations provided higher heat transfer performance.
Adio et al. [290]	Microchannel, Re = 100–700, laminar flow	Al ₂ O ₃ /water (0.5–4 vol.%)	A 43.6% enhancement in heat transfer coefficient was observed.
Adio et al. [291]	Microchannel, Re = 100–400, laminar flow	CuO/Water (0.5–4 vol.%)	A 6.5% enhancement in heat transfer was observed.
Ali et al. [292]	Microchannel, Re = 100–350, laminar flow	Al ₂ O ₃ /water (0–3 vol.%)	The Nusselt number at 3 vol.% and Re = 350 showed a 0.67% enhancement.
Kumar et al. [293]	Microchannel, Re = 200–600, laminar flow	Al ₂ O ₃ /water (0.25–0.75 vol.%)	A 40% heat transfer coefficient enhancement was observed at 0.75 vol.% fraction.
Elbadawy and Fayed [294]	Microchannel, Re = 200–1500, laminar flow	Al ₂ O ₃ /water (0.01–0.05 vol.%)	Cooling performance was enhanced.
Kahani [295]	Microchannel, Re = 100–300, laminar flow	Al ₂ O ₃ /water (0–1 vol.%)	The average Nusselt number increased to 1.36 at a 1 vol.% fraction.
Pourfattah et al. [296]	Microchannel, Re = 25–100, laminar flow	CuO/water (0.02–0.04 vol.%)	The heat transfer coefficient was highest at a 0.04 vol.% fraction.
Kumar et al. [297]	Microchannel, Re = 100–500, laminar flow	Al ₂ O ₃ /water (2–7 vol.%), D = 10–40 nm	Nu increased and thermal resistance decreased when the nanoparticles diameter was reduced.
Arjun and Rakesh [298]	Microchannel, turbulent flow	Al ₂ O ₃ /water (0–5 vol.%)	The heat transfer coefficient improved by about 12% to 5% particle volume fraction.
Reddy et al. [299]	Microchannel, Re = 100–700, laminar flow	CuO/water (0–4 vol.%)	The heat transfer coefficient and viscosity increased, while the specific heat capacity decreased.
Darzi et al. [300]	Straight-tube HEX	Al ₂ O ₃ /water	The heat transfer increased with the concentration.
Maddah et al. [301]	Straight, twisted tape	Al ₂ O ₃ /water	The heat transfer was enhanced by 12% to 52% compared to the tube with twisted tapes.
Sarafraz and Hormozi [302]	Straight	Silver/EG–water (0.1–1 vol.%)	The 0.1–1 vol.% fraction increased the heat transfer coefficient by 22–67%.
Jafarimoghaddam et al. [303]	Straight	Cu/oil	The heat transfer coefficient increased by 17.32%.
Shirvan et al. [304]	Straight	Al ₂ O ₃ /water, $\phi = 0.03$	The Nusselt number was enhanced by 57.7% with Re = 150 and $\phi = 0.03$.
Akyurek et al. [305]	Wire coil turbulator	Al ₂ O ₃ /water	The addition of a wire coil increased the Nusselt number and the heat transfer coefficient.
Albadr et al. [306]	Shell-and-tube HEX	Al ₂ O ₃ /water, $\phi = 2$ v%	The overall heat transfer coefficient increased by 57%.
Godson et al. [307]	Shell-and-tube HEX	Ag/water, $\phi = 0.01$ –0.04 vol.%	There was a 12.4% rise in heat transfer coefficient.
Dharmalingam et al. [308]	Shell-and-tube HEX	Al ₂ O ₃ /water	There was a 17% rise in overall heat transfer coefficient.

Table 7. Cont.

Author(s)	Operating Variables	Nanofluid Characteristics	Findings
Aghabozorg et al. [309]	Shell-and-tube HEX	Fe ₂ O ₃ -CNT/water (0.2 wt.%)	There were 34.02% and 37.50% increases in the heat transfer coefficient for laminar and turbulent flow.
Tan et al. [310]	Shell-and-tube HEX	MWCNT/DI water, $\varphi = 0.2\text{--}1$ wt.%	There was a 24.3% increase in the heat transfer coefficient.
Naik and Vinod [311]	Shell-and-tube HEX	Fe ₂ O ₃ , CuO, Al ₂ O ₃ /(CMC), $\varphi = 1$ wt.%	There were 26% and 29% increases in the overall heat transfer coefficient for Al ₂ O ₃ and CuO nanofluids.
Said et al. [312]	Shell-and-tube HEX	CuO/water	A 7% increase in overall heat transfer and a 11.39% increase in convective heat transfer were observed.

Table 8. Quantitative data of Nusselt number for different fluids.

T (°C)	Water	TiO ₂ (0.1 vol.%)	Al ₂ O ₃ (0.1 vol.%)
10	10.11	10.19	10.48
15	11.05	11.35	12.21
20	12.27	12.68	13.89
25	14.35	14.97	16.71

The survey revealed that many empirical relations are available for calculating the Nusselt number on the basis of nondimensional numbers, i.e., Reynolds and Prandtl numbers. However, the Nusselt number, by definition, depends on the thermal conductivity, geometric parameters, and heat transfer coefficient. Therefore, it is suggested to validate the results in two ways. For this purpose, conducting experiments and obtaining the required parameters are recommended. The table depicts the Nusselt number for base fluid, titania nanofluid, and alumina nanofluid at different temperatures. It can be observed that the Nusselt number increases with the addition of nanoparticles and the increase in working temperature. Hybrid nanofluid plays an extraordinary role in heat transmission in the presence of a magnetic field. The temperature transfer rate increases as the Prandtl number increases. When the surface stretching rate increases, the velocity profile decays while the temperature profile increases [313].

6. Exergy Analysis of Mono/Hybrid Nanofluids

When the conversion of heat energy into valuable work is incomplete, this indicates the presence of unavailable power. The amount of available energy is termed exergy. The exergy increases as the operating condition moves far from the ambient temperature. Hence, for every thermal system where heat and work transfer are essential, one must estimate the exergy, irreversibility, exergetic efficiency, etc. Bhattad et al. [48] performed exergy destruction analysis in their research using different nanoparticle combinations for coolant purposes. Bhattad et al. [101] analyzed exergy destruction with alumina and multiwalled carbon nanotubes. They observed that the irreversibility increased with flow rate and decreased with inlet temperature, as it was directly proportional to flow rate and inversely proportional to inlet temperature. Exergetic efficiency showed the opposite trend. Bhattad et al. [314,315] performed exergy destruction analysis with different brine solution-based fluids and nanoparticle combinations for low-temperature applications. They used working fluid as a secondary refrigerant in plate evaporators. The irreversibility and nondimensional exergy destruction (NDE) were reduced while using brine-based hybrid nanofluids as a secondary refrigerant compared with the corresponding base fluid

for all low-temperature applications. Hybrid nanofluids enhanced the exergetic efficiency and irreversibility distribution ratio (IDR). The irreversibility/exergy destruction of the system can be calculated as follows:

$$I = T_e S_{gen}, \quad (5)$$

where T_e is the ambient temperature in Kelvin.

S_{gen} is the entropy generation rate, which can be calculated as follows:

$$S_{gen} = \dot{m} \left[c_p \ln \left(\frac{T_o}{T_i} \right) + \frac{\Delta p}{\rho T_{av}} \right], \quad (6)$$

where T_{av} is the average temperature of the inlet and outlet temperature.

The second law of efficiency or exergy efficiency (η_{II}) is the ratio of exergy gain to exergy loss, which is given by

$$\eta_{II} = \frac{E_g}{E_l}. \quad (7)$$

The scaling of exergetic parameters has become essential from the design point of view for thermal systems. Hence, different parameters such as non-dimensional exergy destruction, irreversibility distribution ratio, and Bejan number are discussed in the present investigation. Non-dimensional exergy destruction (NDE) is the ratio of irreversibility to maximum heat transfer rate, which signifies the effect of design parameters on the exergy destruction for a given operating condition. A non-dimensional parameter, entropy generation number, was introduced by Mishra et al. [316] to study the influence of heat capacity on entropy generation. The sustainability of the device was evaluated in terms of the exergy ratio to understand the utilization of resources [317]. Bejan [318] introduced the irreversibility distribution ratio (IDR) concept to show the relative influence of heat transfer and pressure drop on irreversibility. The irreversibility distribution ratio was defined as the ratio of entropy generation due to heat transfer to that due to pressure drop.

Bhattad et al. [211] performed exergetic analyses of the plate heat exchanger using Al_2O_3 - TiO_2 hybrid nanofluid as a coolant for sub-ambient temperature application. They observed a 4.01% reduction in the exergetic efficiency for TiO_2 nanofluid. The study showed that the exergetic performance decreased continuously with the increase in TiO_2 ratio in the hybrid solution. Bhattad et al. [212] observed that the irreversibility was enhanced with the flow rate and nanoparticle suspension for MgO -alumina hybrid nanofluid. Bhattad et al. [213] observed an augmentation of the coolant exergy rate, irreversibility rate, and non-dimensional exergy by 4.8%, 7.5%, and 3.5%, respectively. At the same time, the second law of efficiency is reduced when using nanoparticles and increasing flow rate, and it decreases with the coolant inlet temperature. The authors of [319] investigated a novel nanofluid ternary hybrid nanofluid (THdNF) obtained from a mixture of three different nanoparticles, resulting in better overall performance even at low concentrations. Bahiraei et al. [320] examined twisted turbulator inserts in the concurrent pipe and found lower entropy generation when arranged counter-currently. Bahiraei and Heshmatian [321] investigated the effect of nanofluid on the cooling devices on the entropy generation and revealed a net reduction in the temperature. In the interim, various research studies focusing on entropy and exergy investigation are available in the open literature using different nanofluids [322–324]. Kumar and Sahoo [325,326] investigated combined exergo-economic and environmental impact analysis of THdNF as the working fluid with various turbulator inserts used for automobile applications. They found the highest 24.7% exergy change and 6.4% exergy efficiency at the lowest Reynolds number without inserts. Rai and Sahoo [327] performed exergy analysis for a 5% water in diesel emulsion (WiDE) fuel, with 50 ppm carbon nanotube (CNT) and 50 ppm aluminum oxide (Al_2O_3) nano-additive fuels, on a diesel engine with changeable engine speed and load. The exergy-based sustainability was highest for 5% WiDE-CNT fuel at 2000 engine rpm with full engine load. The exergy destruction and entropy generation rates with the 5% WiDE- Al_2O_3 and 5% WiDE-CNT

nano additive fuels had 2.07% and 4.15% higher values, respectively, compared to the diesel fuel.

7. Applications of Mono/Hybrid Nanofluids

Due to their improved thermophysical characteristics, nanofluids and hybrid nanofluids can be used in radiators (as coolant), biodiesel blends, fuel additives, refrigerators, heat pumps, and air conditioning applications as primary fluids (nano refrigerants) and secondary fluids (secondary refrigerants on the evaporator side and nano lubricants as refrigerants on the condenser side). The thermophysical characteristics, pressure drop, and heat transfer characteristics of nano lubricants and nano refrigerants in refrigeration systems were reviewed by Saidur et al. [328] and Bhattad et al. [329]. Alawi et al. [330] discovered that the thermal conductivity of nano refrigerants during pool boiling is highly influenced by the temperature at low concentrations. The properties, flow characteristics, and uses of nano refrigerants at sub-ambient temperatures were evaluated by Celen et al. [331]. The use of nano lubricants and nano refrigerants has been considered in refrigeration, air conditioning, and heat pump systems [332]. The effects of employing nano coolants on cooling devices in terms of energy consumption and heat transfer efficiency were reviewed by Alawi et al. [333]. A review was conducted on the thermophysical characteristics and effectiveness of nano refrigerants in refrigeration systems [334]. Nano refrigerants were thoroughly evaluated by Nair et al. [335], who covered their manufacture, characteristics, heat transfer abilities, and effects on the performance of refrigeration systems. Hybrid nano lubricants were utilized by Zawawi et al. [336] to enhance the performance of refrigeration systems. ZnO/water (0.5 vol.%) nanofluid was described by Fard et al. [337] as the hot fluid in a plate heat exchanger. They demonstrated that the heat transfer behavior of the nanofluid was superior to that of the basic fluid. Javadi et al. [338] looked into how utilizing Al₂O₃, TiO₂, and SiO₂ nanofluids affected the heat transfer of a plate heat exchanger. The SiO₂ nanofluid exhibited a lower pressure drop, while the Al₂O₃ nanofluid had the highest heat transfer coefficient. The thermal characteristics of the two nanofluids were contrasted in a plate heat exchanger operating at low temperatures [339]. Carbon nanotubes and aluminum oxide outperformed water in terms of increased heat transfer and reduced pump power loss.

Nanofluids can be utilized in auxiliary circuits as additional fluids (evaporators and condensers) to cool the primary working fluid or refrigerant [340]. When employing nanofluids, Liu et al. [341] noticed a rise in cooling capacity and COP, as well as a fall in compressor performance. The enhanced HTC enhanced the cooling capacity [342]. Nanofluids were explored numerically by Loaiza et al. [343] for application as secondary coolants in cooling systems. It was discovered that when the concentration of nanoparticles increased and the size of the nanoparticles decreased, the evaporator area and pressure drop of the refrigerant decreased for a specific cooling capacity. Nanofluids had a minimal effect on pump power and increased chiller efficiency, cooling capacity, and efficiency. The use of Cu–H₂O nanofluids as condenser coolant in a vapor compression heat pump was modeled by Parise and Tiecher [344]. A nanoparticle percentage of 2.0% resulted in a 5.4% increase in the efficiency factor. Askari et al. [345] conducted an experimental investigation on the effectiveness of counter flow wet coolers. Nanoporous graphene nanofluids and MWCNTs are employed. They noticed increases in cooling distance, coolant flow, and cooling tower efficiency. When Kolhapure and Patil [346] employed nanofluids as refrigerants, they found that compressor operation and condenser heat transfer decreased as efficiency increased. Condensers and cooling tower sizes were reduced.

Thermal simulations of vapor compression refrigeration systems were detailed by Jaiswal and Mishra [347] utilizing Al₂O₃-, TiO₂-, CuO-, and Cu-based nanofluids in the secondary circuit and R134a refrigerant in the primary circuit. Using aqueous nanofluids in the secondary circuit boosted system performance with the same geometrical parameters from 17% to 20%. Increased cold chain efficiency employing nanofluids as secondary refrigerants was reported by Ndoye et al. [348]. To investigate the energy characteristics

of secondary circuits in refrigeration systems, Soliman et al. [349] employed a variety of nanofluids. It was noted that, when concentration increased, the pump power increased, whereas the performance coefficient decreased. Excellent cooling capacity and COP for SWCNT/water suspensions were reported by Vasconcelos et al. [350]. In air conditioning systems, nanofluids can be employed as phase change refrigeration reservoirs on the evaporator side [351]. Nanotechnology is widely used in the food, food packaging, and milk pasteurization industries [352]. Zhang et al. [353] examined the ice formation process' nucleation phenomenon using nanofluids. With nanofluids, the nucleation mechanism could be improved. A raw milk dispenser based on nanofluidic technology was created by Longo et al. [354]. Hybrid nanofluids were employed as secondary coolants for low-temperature applications by Bhattad et al. [314,315,355]. Table 9 provides an overview of the uses of nanofluids as primary and secondary coolants.

Table 9. Summary of the application of nanofluids as coolant and secondary refrigerant.

Author(s)	Operating Variables	Nanofluid Characteristics	Findings
Liu et al. [341]	MWCNT/water,	Water chiller	Efficiency improved by 5.15%, while cooling capacity increased by 4.2%.
Loaiza et al. [343]	Al ₂ O ₃ , TiO ₂ , CuO, and Cu/water	Vapor compression refrigeration system	The evaporator area and pressure drop decreased for fixed cooling capacity as particle size and concentration increased.
Zhang et al. [353]	Al ₂ O ₃ , SiO ₂ /water	Ice making	With the use of nanoparticles, supercooling was reduced to a lesser extent.
Kumaresan et al. [342]	MWCNT/(EG + water)	-	Higher temperatures and velocities increased heat transmission efficiency, preferably with 0.15% MWCNTs by volume.
Parise and Tiecher [344]	Cu/water	Vapor compression heat pumps	When the volume fraction of nanoparticles reached 2%, COP increased by 5.4%.
Sarkar [356,357]	Al ₂ O ₃ , TiO ₂ , CuO, SiO ₂ , and Cu/water	CO ₂ refrigerant system	The shell-and-tube gas cooler's cooling effectiveness and capacity were enhanced.
Jaiswal and Mishra [347]	Al ₂ O ₃ , TiO ₂ , CuO, and Cu/water	Domestic refrigeration system	The performance of the cooling system increased by 17–20%.
Longo et al. [354]	Al ₂ O ₃ /(EG + water)	Milk dispenser	Energy consumption was reduced by 63–70%.
Ndoye et al. [348]	Co, CuO, Fe, SiO ₂ , Al ₂ O ₃ , and TiO ₂ /water	Cold chain refrigeration plants	The cold chain became more efficient by consuming less energy and producing fewer emissions.
Askari et al. [345]	MWCNT and graphene/water	Cooling tower	Efficiency, cooling range, and cooling tower performance were all improved with lower water use, as were the tower's attributes.
Kolhapure and Patil [346]	Al ₂ O ₃ /water	Air conditioning and refrigeration system	The capacitor thermal cutoff, which lowered compressor operation and used less energy, boosted COP.
Soliman et al. [349]	Al ₂ O ₃ , Ag, TiO ₂ , Co, Cu, Au, Fe, CuO, diamond, and graphite/water	Refrigeration system	When the mass fraction was 0.1%, productivity increased by 10.5%.
Vasconcelos et al. [350]	SWCNT/water	Vapor compression refrigeration system	Excellent COP and cooling capacity.

Arshad et al. [358] investigated the 3D flow of an engine oil-based nanofluid under the impact of rotation and partial slip phenomenon over a stretchable surface. The study's outcomes were related to already available studies and were in good agreement. Kumar and Sahoo [359] investigated the performance characteristics of a car radiator by using a

ternary hybrid nanofluid of 0.12 vol.% fraction ($\text{Al}_2\text{O}_3\text{-CuO-TiO}_2/\text{water}$) and water as coolant and validated results with simulation. Ternary hybrid nanofluids (THNF) showed a 14% higher heat transfer coefficient at 8 lpm, and the mixture model predicted a 5% better result than the single-phase approach. A 12.54% enhancement in BTE was observed with a fuel-saving rate of 14.28%. Kumar and Sahoo [360] investigated the thermo-hydraulic performance of a car radiator using Al_2O_3 , CuO, and TiO_2 nanoparticles disseminated in an equal fraction in the range of 0.06–0.12% THNF. Coolant was operated with a flow rate of 3–8 lpm. Results revealed a 14.2% enhancement in heat transfer with a coolant flow rate of 6 lpm using a 0.12% vol. fraction of THNF. A maximum fuel saving rate of 14.28% was observed at 50% load on the engine. Preheating of fuel through radiator waste heat recovery decreased the BSFC. Rai and Sahoo [361] investigated the engine performance parameters for 5% water-emulsified fuel, 50 ppm CNT, and 50 ppm $\text{Al}_2\text{O}_3\text{-CNT}$ (25 ppm each) hybrid nano-additive fuels, with different speeds and loads on a DIC I engine. The CNT catalyst had a higher effect on the BSFC than the $\text{Al}_2\text{O}_3\text{-CNT}$ catalyst. The BTE with 5% WiDE, 5% WiDE- $\text{Al}_2\text{O}_3\text{-CNT}$, and 5% WiDE-CNT nano-additive was 1.49%, 2.86%, and 3.07% higher than with diesel. Overall, compared to all fuel blends, the optimal performance was found for 5% WiDE-CNT. Najafi [362] observed the impact of adding Ag and CNT nano-additive on engine performance and combustion parameters. The results showed that adding a nanocatalyst shortened the time needed for the engine to ignite and increased the cylinder's peak pressure and rate of heat release. The best outcome was obtained when 120 ppm of CNT nano-additive is used. Jiaqiang et al. [363] evaluated the effects of adding water and a nanocatalyst on a CI engine's performance and emission characteristics when using diesel/biodiesel mixes. The blend of biodiesel and diesel with 90 ppm CeO_2 nano-additive was emulsified with 2%, 4%, and 6% (*v/v*) ratios. The investigation results showed that water emulsification up to 4% was favorable, and the addition of nanocatalyst enhanced performance and lowered emissions levels. Kumar and Raheman [364] investigated water-emulsified biodiesel blends with nano-oxide incorporation. According to the characterization analysis, the ideal fuel stability characteristics were 1% surfactant, 10% water, 2500 rpm stirrer speed, and 69.7 ppm nano-oxide.

Wroblewski [365,366] performed energy analysis on IC engines for hydrophobic and hydrophilic multilayer nanocoatings surrounded by soot. The multilayer coating reduced the friction coefficient and, hence, improved tribological performance. Rai and Sahoo [367] carried out energy, exergy, and sustainability analyses of a diesel engine with hybrid nanofluids incorporated with various shaped (25 ppm CNT and 25 ppm spherical Al_2O_3 nano-additives). The 5% WiDE based $\text{Al}_2\text{O}_3\text{-CNT}$ hybrid nano fuel improved BTE by 2.86% with an exergy efficiency of 4.16%. Rao and Anand [368] investigated an analysis of the energy and emissions produced by a DIC I engine running on fuel containing AlO(OH) nano-additive and water in a diesel emulsion. The results of the experimental study demonstrated that adding water as an AlO(OH) nano-additive to diesel emulsion fuel considerably enhanced the engine's energy parameters and emission characteristics. El-Seesy et al. [369] examined the optimal Al_2O_3 nano-additive concentration in diesel and Jojoba biodiesel blends to achieve higher performance. The analysis showed that all performance indicators significantly increased at a concentration of 30 mg/L Al_2O_3 . Ozcan [370] studied the impact of Al_2O_3 nano-additive (50 and 100 ppm) on the energy and performance parameters of diesel engines charged with diesel/biodiesel blends through experiments. According to experimental data, the engine's performance was improved, entropy generation decreased, and unexplained losses decreased. Hasannuddin et al. [371] evaluated the fuel qualities, emission characteristics, and performance metrics of diesel engines running on fuel containing various nano-additives and 10% water (Al_2O_3 , CuO, MgO, MnO, and ZnO). According to the study, of all the nano fuels discussed, the water-in-diesel emulsion with Al_2O_3 addition had the smallest droplet size, improved torque, and decreased BSFC, BSCO, and BSNOx. Aghbashlo et al. [372] performed an energetic performance investigation of the diesel engine using four concentrations of hybrid nanocatalyst and two types of biodiesel/diesel blends (CeO_2 and MWCNT). The results showed

that all fuel mixes had the same energy efficiency and sustainability index except for the nano-catalyst.

8. Conclusions

Investigations were made on different mono and hybrid nanofluids from nanocomposites, mixing other nanoparticles comprising oxides, metals, and phase change materials of different shapes such as spherical, cylindrical, and flake in a base fluid using one-step and two-step methods. Nanofluids were characterized and thermo-physical properties were measured to develop empirical relations for CFD simulations. Experimental and theoretical investigations were conducted on the heat exchangers with mono and hybrid nanofluids, and an enhancement in performance was observed. A study on different hybrid nanofluids (SiC, Al₂O₃–AlN, Al₂O₃–MgO, Al₂O₃–CuO, and Al₂O₃–MWCNT) conducted by Bhattad et al. [210] showed the ranking of different nanofluids according to different thermophysical properties. These nanofluids can serve as a coolant, secondary refrigerant, nano refrigerant, and nano lubricant for low-temperature applications such as refrigeration systems, air conditioning, and food processing, or as fuels for ICEs. From the present literature survey, the research gaps identified are as follows:

- There are limited studies on the heat transfer properties of hybrid nanofluid heat exchangers.
- The influence of individual particle proportions of hybrid nanofluids on the performance of heat exchangers is unknown.
- There is little experimental work and validation by CFD modeling of heat exchangers using hybrid nanofluids operating for low-temperature applications.
- Hybrid nanofluids can be used in biodiesel blends and as fuel additives to enhance the performance of IC engines.
- A single correlation containing the effect of temperature and particle size is needed to predict accurate thermal conductivity and viscosity of mono/hybrid nanofluids.
- Nanofluids with more thermal conductivity show better heat transfer characteristics, and nanofluids with more viscosity provide higher pressure drop and pump work. An increment in heat transfer is desirable, while an increment in pump work is undesirable; thus, another performance indicator must be determined, such as a performance index (ratio of heat transfer rate and pump work), to obtain a better nanofluid.
- Many empirical relations are available for calculating the Nusselt number on the basis of non-dimensional numbers, i.e., Reynolds and Prandtl numbers. However, the Nusselt number, by definition, depends on the thermal conductivity, geometric parameters, and heat transfer coefficient. Hence, it is suggested to validate the results in two ways. For this purpose, conducting the experiments and obtaining the required parameters are recommended.
- It can be observed that the thermal conductivity, density, and viscosity increase with the addition of nanoparticles in the base fluid. The fluid's thermal conductivity increases with the temperature increase, whereas density and viscosity decrease. No change can be observed for the specific heat as the studied temperature range is small.
- Hybrid nanofluids can be used as a coolant in automobile radiators and ICEs.
- Few investigations are available for ternary hybrid nanofluids to analyze irreversibility, exergy, economic, and the second law of efficiency in air heat exchangers utilizing various turbulators.
- Studies were conducted primarily with water and EG/water brine as base fluids. Using different brines as primary and secondary cooling water should be explored.

Most (95%) investigators adopted a two-step method while preparing nanofluids. However, nanofluids synthesized using the one-step process (which is expensive and involved) improved the stability of the nanoparticles in the base fluid due to the high sedimentation rate with low sonification time. Ultrasonication reduces the sedimentation issue, and adding surfactants further improves nanofluid stability. FESEM/EDS, DLS, and zeta potential measurements help understand nanoparticle morphology, shape, and size. The mechanism of nanofluids at the atomic level should be understood to address parti-

cle migration, aggregation, and stability with minimal experimentation. Future research should focus on industrial applications to minimize pressure losses, specify the optimal concentration of nanoparticles, and ensure the long-term stability of hybrid nanofluids. Very few studies are available on ternary hybrid nanofluid to analyze irreversibility, exergy, economic, and the second law of efficiency in air heat exchangers utilizing various turbulators. Thus, this area needs to be explored more to improve automobile performance.

Author Contributions: Conceptualization, A.B., V.A. and N.R.B.; methodology, B.N.R. and V.A.; software, V.A. and R.P.S.; validation, V.A., N.R.B. and C.V.; formal analysis, V.A., N.R.B. and A.B.; investigation, V.A. and R.P.S.; resources, C.V., S.K., T.M.Y.K. and A.M.S.; data curation, V.A., R.P.S. and N.R.B.; writing—original draft preparation, V.A. and B.N.R.; writing—review and editing, V.A., B.N.R. and N.H.A.; visualization, N.H.A., C.V., S.K. and A.M.S.; supervision, V.A. and N.R.B.; project administration, T.M.Y.K., C.V., S.K. and N.R.B.; funding acquisition, T.M.Y.K., C.V. and S.K. All authors have read and agreed to the published version of the manuscript.

Funding: This work was funded by King Khalid University under grant number RGP2/76/44.

Data Availability Statement: Not applicable.

Acknowledgments: The authors extend their appreciation to the Deanship of Scientific Research at King Khalid University for funding this work through large group Research Project under grant number RGP2/76/44.

Conflicts of Interest: The authors declare no conflict of interest.

Nomenclature

b	Plate spacing, mm
C	Specific heat, J/kg·K
K	Thermal conductivity, W/m·K
\dot{m}	Mass flow rate, kg/s
N	Shape factor
Pe	Pecklet number
Re	Reynolds number
T	Temperature, °C
V	Volume, m ³

Abbreviation

COP	Coefficient of performance
CTAB	Cetyl trimethyl ammonium bromide
DI	Deionized water
DLS	Dynamic light scattering
EG	Ethylene glycol
F-CNF	Functionalized carbon nanofiber
FESEM	Field-emission scanning electron microscopy
GA	Gum Arabic
HCFC	Hydrochlorofluorocarbons
HEG	Hydrogen-induced exfoliated graphene
HEX	Heat exchanger
HTC	Heat transfer coefficient
HVAC	Heating, ventilation, and air conditioning
HyNf	Hybrid nanofluid
MCHS	Microchannel heat sink
MWCNT	Multiwalled carbon nanotube
PCM	Phase change material
PHE	Plate heat exchanger
PHP	Pulsating heat pipe
PVP	Polyvinyl pyrrolidone
PVA	Polyvinyl alcohol
rGO	Reduced graphene oxide

SDS	Sodium dodecyl sulfate
SDBS	Sodium dodecyl benzene sulfonate
SEM	Scanning electron microscopy
TEM	Transmission electron microscopy
VSM	Vibrating sample magnetometry
v%	Percentage volume concentration
XRD	X-ray diffraction
Greek symbols	
β	Chevron angle, $^{\circ}$
Ω	Discharge, lpm
μ	Dynamic viscosity, Pa·S
ρ	Density, kg/m ³
Φ	Volume concentration
Ψ	Coefficient
Subscript	
1	First
2	Second
bf	Base fluid
nf	Nanofluid
p	Nanoparticle
eff	Effective
h	Hot
c	Cold
i	Inlet

References

- Rao, V.; Sankar, B. Heat transfer and friction factor investigations of CuO nanofluid flow in a double pipe U-bend heat exchanger. *Mater. Today Proc.* **2019**, *18*, 207–218.
- Omidi, M.; Farhadi, M.; Jafari, M. A comprehensive review on double pipe heat exchangers. *Appl. Therm. Eng.* **2017**, *110*, 1075–1090. [[CrossRef](#)]
- Li, H.; Wang, Y.; Han, Y.; Li, W.; Yang, L.; Guo, J.; Liu, Y.; Zhang, J.; Zhang, M.; Jiang, F. A comprehensive review of heat transfer enhancement and flow characteristics in the concentric pipe heat exchanger. *Powder Technol.* **2021**, *397*, 117037. [[CrossRef](#)]
- Ding, M.; Liu, C.; Rao, Z. Experimental investigation on heat transfer characteristic of TiO₂-H₂O nanofluid in microchannel for thermal energy storage. *Appl. Therm. Eng.* **2019**, *160*, 114024. [[CrossRef](#)]
- Alshukri, M.; Hussein, A.; Eidan, A.; Alsabery, A. A review on applications and techniques of improving the performance of heat pipe-solar collector systems. *Sol. Energy* **2022**, *236*, 417–433. [[CrossRef](#)]
- Cengel, Y. *Heat and Mass Transfer. A Practical Approach*, 3rd ed.; McGraw Hill/Interamericana Editores, S.A.: Mexico City, Mexico, 2013; pp. 1689–1699.
- Rostami, S.; Shahsavari, A.; Kefayati, G.; Goldanlou, A.S. Energy and exergy analysis of using turbulator in a parabolic trough solar collector filled with mesoporous silica modified with copper nanoparticles hybrid nanofluid. *Energies* **2020**, *13*, 2946. [[CrossRef](#)]
- Choi, S. *Enhancing Thermal Conductivity of Fluids with Nanoparticles, Developments and Applications of Non-Newtonian Flows*; ASME: New York, NY, USA, 1995; pp. 99–105.
- Kumar, P.M.; Palanisamy, K.; Vijayan, V. Stability analysis of heat transfer hybrid/water nanofluids. *Mater. Today Proc.* **2020**, *21*, 708–712. [[CrossRef](#)]
- Okonkwo, E.; Wole-Osho, I.; Almanassra, I.; Abdullatif, Y.; Al-Ansari, T. An updated review of nanofluids in various heat transfer devices. *J. Therm. Anal.* **2021**, *145*, 2817–2872. [[CrossRef](#)]
- Sarkar, J.; Ghosh, P.; Adil, A. A review on hybrid nanofluids: Recent research, development and applications. *Renew. Sustain. Energy Rev.* **2015**, *43*, 164–177. [[CrossRef](#)]
- Sahin, A. Performance enhancement of solar energy using nanofluids: An update review. *Renew Energy* **2020**, *145*, 1126–1148. [[CrossRef](#)]
- Zayed, M.; Du, Y.; Kabeel, A.; Shalaby, S. Factors affecting the thermal performance of the plate solar collector using nanofluids: A review. *Sol. Energ.* **2019**, *182*, 382–396. [[CrossRef](#)]
- Wahab, A.; Hassan, A.; Qasim, M.; Ali, H.; Babar, H.; Sajid, M. Solar energy systems—Potential of nanofluids. *J. Mol. Liq.* **2019**, *289*, 111049. [[CrossRef](#)]
- Pordanjani, A.; Aghakhani, S.; Afrand, M.; Mahmoudi, B.; Mahian, O.; Wongwises, S. An updated review on application of nanofluids in heat exchangers for saving energy. *Energy Convers. Manag.* **2019**, *198*, 111886. [[CrossRef](#)]
- Sajid, M.; Ali, H. Recent advances in application of nanofluids in heat transfer devices: A critical review. *Renew. Sustain. Energy Rev.* **2019**, *103*, 556–592. [[CrossRef](#)]

17. Kumar, A.; Subudhi, S. Preparation, characterization and heat transfer analysis of nanofluids used for engine cooling. *Appl. Therm. Eng.* **2019**, *160*, 114092. [[CrossRef](#)]
18. Rahman, S.; Ashraf, M.; Amin, A.; Bashir, M.; Ashik, M.; Kamruzzaman, M. Tuning nanofluids for improved lubrication performance in turning biomedical grade titanium alloy. *J. Clean. Prod.* **2019**, *206*, 180–196. [[CrossRef](#)]
19. Panithasan, M.; Gopalakichenin, D.; Veeraraagavan, S. Impact of rice husk nanoparticle on the performance and emission aspect of a diesel engine running on blends on pine oildiesel. *Env. Sci. Pollut. Res.* **2019**, *26*, 282–291. [[CrossRef](#)]
20. Pinto, R.; Fiorelli, F. Review of the mechanisms responsible for heat transfer enhancement using nanofluids. *Appl. Therm. Eng.* **2016**, *108*, 720–739. [[CrossRef](#)]
21. Radomska, E.; Mika, L.; Sztokler, K. The impact of additives on the main properties of phase change materials. *Energies* **2020**, *13*, 3064. [[CrossRef](#)]
22. Suhaimi, N.; Din, M.; Hamid, M.; Amin, N.; Zamri, W.; Wang, J. Optimum electrical and dielectric performance of multi-walled carbon nanotubes doped disposed transformer oil. *Energies* **2020**, *13*, 3181. [[CrossRef](#)]
23. Sekar, A.; Jayabalan, T.; Muthukumar, H.; Chandrasekaran, N.; Mohamed, S.; Matheswaran, M. Enhancing power generation and treatment of dairy waste water in microbial fuel cell using Cu-doped iron oxide nanoparticles decorated anode. *Energy* **2019**, *172*, 173–180. [[CrossRef](#)]
24. Said, Z.; Gupta, M.; Khan, A.; Jamil, M.; Bellos, E. A comprehensive review on minimum quantity lubrication (MQL) in machining processes using nano-cutting fluids. *Int. J. Adv. Manuf. Technol.* **2019**, *105*, 2057–2086. [[CrossRef](#)]
25. Humnic, G.; Humnic, A. The influence of hybrid nanofluids on the performances of elliptical tube: Recent research and numerical study. *Int. J. Heat Mass Transf.* **2019**, *129*, 132–143. [[CrossRef](#)]
26. Elsaid, A. Experimental study on the heat transfer performance and friction factor characteristics of Co_3O_4 and Al_2O_3 based $\text{H}_2\text{O}/(\text{CH}_2\text{OH})_2$ nanofluids in a vehicle engine radiator. *Int. Commun. Heat Mass Transf.* **2019**, *108*, 104263. [[CrossRef](#)]
27. Al-Shdaifat, M.; Zulkifli, R.; Sopian, K.; Salih, A. Thermal and hydraulic performance of CuO/water nanofluids: A review. *Micromachines* **2020**, *11*, 416. [[CrossRef](#)] [[PubMed](#)]
28. Eshgarf, H.; Kalbasi, R.; Maleki, A.; Shadloo, M.; Karimipour, A. A review on the properties, preparation, models and stability of hybrid nanofluids to optimize energy consumption. *J. Therm. Anal. Calorim.* **2021**, *144*, 1959–1983. [[CrossRef](#)]
29. Zainon, S.; Azmi, W. Recent progress on stability and thermo-physical properties of mono and hybrid towards green nanofluids. *Micromachines* **2021**, *12*, 176. [[CrossRef](#)] [[PubMed](#)]
30. Pavia, M.; Alajami, K.; Estellé, P.; Vigolo, B. A critical review on thermal conductivity enhancement of graphene-based nanofluids. *Adv. Colloid. Interface Sci.* **2021**, *294*, 102452. [[CrossRef](#)] [[PubMed](#)]
31. Inlow, S.; Groll, E. A performance comparison of secondary refrigerants. In Proceedings of the 1996 Purdue International Refrigeration Conference, West Lafayette, IN, USA, 23 July 1996; pp. 167–178.
32. Wang, K.; Eisele, M.; Hwang, Y.; Radermacher, R. Review of secondary loop refrigeration systems. *Int. J. Refrig.* **2010**, *33*, 212–234. [[CrossRef](#)]
33. Sreelakshmy, K.; Aswathy, S.; Vidhya, K.; Saranya, T.; Sreeja, C. An overview of recent nanofluid research. *Int. Res. J. Pharm.* **2014**, *5*, 239–243.
34. Nor-Azwadi, C.; Adamu, I.; Jamil, M. Preparation methods and thermal performance of hybrid nanofluids. *J. Adv. Rev. Sci. Res.* **2016**, *24*, 13–23.
35. Sidik, N.; Adamu, I.; Jamil, M.; Kefayati, G.; Mamat, R.; Najafi, G. Recent progress on hybrid nanofluids in heat transfer applications: A comprehensive review. *Int. Commun. Heat Mass Transf.* **2016**, *78*, 68–79. [[CrossRef](#)]
36. Nabil, M.; Azmi, W.; Hamid, K.; Zawawi, N.; Priyandoko, G.; Mamat, R. Thermo-physical properties of hybrid nanofluids and hybrid nanolubricants: A comprehensive review on performance. *Int. Commun. Heat Mass Transf.* **2017**, *83*, 30–39. [[CrossRef](#)]
37. Sundar, L.; Sharma, K.; Singh, M.; Sousa, A. Hybrid nanofluids preparation, thermal properties, heat transfer and friction factor—A review. *Renew. Sustain. Energy Rev.* **2017**, *68*, 185–198. [[CrossRef](#)]
38. Babu, J.; Kumar, K.; Rao, S. State-of-art review on hybrid nanofluids. *Renew. Sustain. Energy Rev.* **2017**, *77*, 551–565. [[CrossRef](#)]
39. Sidik, N.; Jamil, M.; Aziz-Japar, W.; Adamu, I. A review on preparation methods, stability and applications of hybrid nanofluids. *Renew. Sustain. Energy Rev.* **2017**, *80*, 1112–1122. [[CrossRef](#)]
40. Kumar, D.; Arasu, A. A comprehensive review of preparation, characterization, properties and stability of hybrid nanofluids. *Renew. Sustain. Energy Rev.* **2018**, *81*, 1669–1689. [[CrossRef](#)]
41. Gupta, M.; Singh, V.; Kumar, S.; Said, Z. Up to date review on the synthesis and thermophysical properties of hybrid nanofluids. *J. Clean. Prod.* **2018**, *190*, 169–192. [[CrossRef](#)]
42. Jamkhande, P.; Bamer, A.; Kalaskar, M. Metal nanoparticles synthesis: An overview on methods of preparation, advantages and disadvantages, and applications. *J. Drug Deliv. Sci. Technol.* **2019**, *53*, 101174. [[CrossRef](#)]
43. Asadi, A.; Aberoumand, S.; Moradikazerouni, A.; Pourfattah, F.; Żyła, G.; Estellé, P.; Mahian, O.; Wongwises, S.; Nguyen, H.M.; Arabkoohsar, A. Recent advances in preparation methods and thermophysical properties of oil-based nanofluids: A state of the art review. *Powder Technol.* **2019**, *352*, 209–226. [[CrossRef](#)]
44. Arshad, A.; Jabbal, M.; Yan, Y.; Reay, D. A review on graphene based nanofluids: Preparation, characterization and applications. *J. Mol. Liq.* **2019**, *279*, 444–484. [[CrossRef](#)]
45. Mishra, P.; Sen, S.; Amin, R.; Biring, S. Effect of annealing on structure, optoelectronic and photoresponsivity properties of sol-gel prepared ZnO nanoparticles. *Mater. Today Proc.* **2019**, *17*, 261–265. [[CrossRef](#)]

46. Esmaeili, E.; Rounaghi, S.; Gruner, W.; Eckert, J. The preparation of surfactant-free highly dispersed ethylene glycol-based aluminum nitride-carbon nanofluids for heat transfer application. *Adv. Powder Technol.* **2019**, *30*, 2032–2041. [[CrossRef](#)]
47. Das, N.; Naik, P.; Reddy, D.; Mallik, B.; Bose, S.; Banerjee, T. Experimental and molecular dynamic insights on the thermophysical properties for MWCNT-Phosphonium based eutectic thermal media. *J. Mol. Liq.* **2022**, *354*, 118892.
48. Bhattad, A.; Sarkar, J.; Ghosh, P. Use of Hybrid Nanofluids in Plate Heat Exchanger for Low Temperature Applications. Ph.D. Thesis, Indian Institute of Technology Banaras Hindu University, Varanasi, Uttar Pradesh, India, 2019.
49. Jana, S.; Khojin, A.; Zhong, W. Enhancement of fluid thermal conductivity by the addition of single and hybrid nano-additives. *Thermochim. Acta* **2007**, *462*, 45–55. [[CrossRef](#)]
50. Han, Z.; Yang, B.; Kim, S.; Zachariah, M. Application of hybrid sphere/ carbon nanotube particles in nanofluids. *Nanotechnology* **2007**, *18*, 105701. [[CrossRef](#)]
51. Turcu, R.; Pana, O.; Nan, A.; Craciunescu, I.; Chauvet, O.; Payen, C. Polypyrrole coated magnetite nanoparticles from water based nanofluids. *J. Phys. Appl. Phys.* **2008**, *41*, 245002. [[CrossRef](#)]
52. Jha, N.; Ramaprabhu, S. Synthesis and thermal conductivity of copper nanoparticle decorated multiwalled carbon nanotubes based nanofluids. *J. Phys. Chem. C* **2008**, *112*, 9315–9319. [[CrossRef](#)]
53. Han, W.; Rhi, S. Thermal characteristics of grooved heat pipe with hybrid nanofluids. *Therm. Sci.* **2011**, *15*, 195–206. [[CrossRef](#)]
54. Baby, T.; Sundara, R. Synthesis and transport properties of metal oxide decorated graphene dispersed nanofluids. *J. Phys. Chem. C* **2011**, *115*, 8527–8533. [[CrossRef](#)]
55. Paul, G.; Philip, J.; Raj, B.; Das, P.; Manna, I. Synthesis, characterization and thermal property measurement of nano-Al95Zn05 dispersed nanofluid prepared by a two-step process. *Int. J. Heat Mass Transf.* **2011**, *54*, 3783–3788. [[CrossRef](#)]
56. Suresh, S.; Venkataraj, K.; Selvakumar, P.; Chandrasekar, M. Synthesis of Al₂O₃-Cu/water hybrid nanofluids using two step method and its thermo physical properties. *Colloids Surfaces A Physicochem. Eng. Asp.* **2011**, *388*, 41–48. [[CrossRef](#)]
57. Botha, S.S.; Ndungu, P.; Bladergroen, B.J. Physicochemical properties of oil-based nanofluids containing hybrid structures of silver nanoparticles supported on silica. *Ind. Eng. Chem. Res.* **2011**, *50*, 3071–3077. [[CrossRef](#)]
58. Ho, C.; Huang, J.; Tsai, P.; Yang, Y. On laminar convective cooling performance of hybrid water-based suspensions of Al₂O₃ nanoparticles and MEPCM particles in a circular tube. *Int. J. Heat Mass Transf.* **2011**, *54*, 2397–2407. [[CrossRef](#)]
59. Baby, T.; Sundara, R. Synthesis and nanofluid application of silver nanoparticles decorated graphene. *J. Mater. Chem.* **2011**, *21*, 9702–9709. [[CrossRef](#)]
60. Amiri, A.; Shanbedi, M.; Eshghi, H.; Heris, S.; Baniadam, M. Highly dispersed multiwalled carbon nanotubes decorated with Ag nanoparticles in water and experimental investigation of the thermophysical properties. *J. Phys. Chem. C* **2012**, *116*, 3369–3375. [[CrossRef](#)]
61. Chen, L.; Yu, W.; Xie, H. Enhanced thermal conductivity of nanofluids containing Ag/MWNT composites. *Powder Technol.* **2012**, *231*, 18–20. [[CrossRef](#)]
62. Aravind, S.; Ramaprabhu, S. Graphene wrapped multiwalled carbon nanotubes dispersed nanofluids for heat transfer applications. *J. Appl. Phys.* **2012**, *112*, 124304–124309. [[CrossRef](#)]
63. Bhosale, G.; Borse, S. Pool boiling CHF enhancement with Al₂O₃-CuO/H₂O hybrid nanofluid. *Int. J. Eng. Res. Technol.* **2013**, *2*, 946–950.
64. Balla, H.; Abdullah, S.; MohdFaizal, W.; Zulkifli, R.; Sopian, K. Numerical study of the enhancement of heat transfer for hybrid CuO-Cu nanofluids flowing in a circular pipe. *J. Oleo Sci.* **2013**, *62*, 533–539. [[CrossRef](#)]
65. Abbasi, S.; Rashidi, A.; Nemati, A.; Arzani, K. The effect of functionalisation method on the stability and the thermal conductivity of nanofluid hybrids of carbon nanotubes/gamma alumina. *Ceram. Int.* **2013**, *39*, 3885–3891. [[CrossRef](#)]
66. Nine, M.; Munkhbayar, B.; Rahman, M.; Chung, H.; Jeong, H. Highly productive synthesis process of well dispersed Cu₂O and Cu/Cu₂O nanoparticles and its thermal characterization. *Mater. Chem. Phys.* **2013**, *141*, 636–642. [[CrossRef](#)]
67. Munkhbayar, B.; Tanshen, M.; Jeoun, J.; Chung, H.; Jeong, H. Surfactant-free dispersion of silver nanoparticles into MWCNT-aqueous nanofluids prepared by one-step technique and their thermal characteristics. *Ceram. Int.* **2013**, *39*, 6415–6425. [[CrossRef](#)]
68. Sundar, L.; Singh, M.; Ramana, E.; Sing, B.; Gracio, J.; Sousa, A. Enhanced thermal conductivity and viscosity of nanodiamond-nickel nanocomposite nanofluids. *Sci. Rep.* **2014**, *4*, 4039. [[CrossRef](#)]
69. Parameshwaran, R.; Deepak, K.; Saravanan, R.; Kalaiselvam, S. Preparation, thermal and rheological properties of hybrid nanocomposite phase change material for thermal energy storage. *Appl. Energy* **2014**, *115*, 320–330. [[CrossRef](#)]
70. Batmunkh, M.; Tanshen, M.; Nine, M.; Myekhlai, M.; Choi, H.; Chung, H.; Jeong, H. Thermal conductivity of TiO₂ nanoparticles based aqueous nanofluids with an addition of a modified silver particle. *Ind. Eng. Chem. Res.* **2014**, *53*, 8445–8451. [[CrossRef](#)]
71. Madhesh, D.; Parameshwaran, R.; Kalaiselvam, S. Experimental investigation on convective heat transfer and rheological characteristics of Cu-TiO₂ hybrid nanofluids. *Exp. Therm. Fluid Sci.* **2014**, *52*, 104–115. [[CrossRef](#)]
72. Chen, L.; Cheng, M.; Yang, D.; Yang, L. Enhanced thermal conductivity of nanofluid by synergistic effect of multi-walled carbon nanotubes and Fe₂O₃ nanoparticles. *Appl. Mech. Mater.* **2014**, *548*, 118–123.
73. Parekh, K. Thermo-magnetic properties of ternary polydispersed Mn_{0.5}Zn_{0.5}Fe₂O₄ ferrite magnetic fluid. *Solid State Commun.* **2014**, *187*, 33–37. [[CrossRef](#)]
74. Luo, T.; Wei, X.; Zhao, H.; Cai, G.; Zheng, X. Tribology properties of Al₂O₃/TiO₂ nanocomposites as lubricant additives. *Ceram. Int.* **2014**, *40*, 10103–10109. [[CrossRef](#)]

75. Madhesh, D.; Kalaiselvam, S. Experimental study on heat transfer and rheological characteristics of hybrid nanofluids for cooling applications. *J. Exp. Nanosci.* **2015**, *10*, 1194–1213. [[CrossRef](#)]
76. Zubir, M.; Badarudin, A.; Kazi, S.; Huang, N.; Misran, M.; Sadeghinezhad, E.; Mehrali, M.; Syuhada, N.; Gharehkhani, S. Experimental investigation on the use of reduced graphene oxide and its hybrid complexes in improving closed conduit turbulent forced convective heat transfer. *Exp. Therm. Fluid Sci.* **2015**, *66*, 290–303. [[CrossRef](#)]
77. Qadri, M.; Chandra, R.; Ravindra, S.; Velmurugan, V. Synthesis and testing of graphene /cuprous oxide composite based nano fluids for engine coolants. *Mater. Today Proc.* **2015**, *2*, 4640–4645. [[CrossRef](#)]
78. Karimi, A.; Sadatlu, M.; Saberi, B.; Shariatmadar, H. Experimental investigation on thermal conductivity of water based nickel ferrite nanofluids. *Adv. Powder Technol.* **2015**, *26*, 1529–1536. [[CrossRef](#)]
79. Chakraborty, S.; Sarkar, I.; Haldar, K.; Pal, S.; Chakraborty, S. Synthesis of Cu–Al layered double hydroxide nanofluid and characterization of its thermal properties. *Appl. Clay Sci.* **2015**, *107*, 98–108. [[CrossRef](#)]
80. Megatiff, L.; Ghozatloo, A.; Arimi, A.; Niasar, M. Investigation of laminar convective heat transfer of a novel TiO₂-carbon nanotube hybrid water-based nanofluid. *Exp. Heat Transf.* **2015**, *6152*, 1–15. [[CrossRef](#)]
81. Abbasi, S.; Zebajrad, S.; Baghban, S.; Youssefi, A.; Ekrami-Kakhki, M. Experimental investigation of the rheological behavior and viscosity of decorated multi-walled carbon nanotubes with TiO₂ nanoparticles/water nanofluids. *J. Therm. Anal. Calorim.* **2016**, *123*, 81–89. [[CrossRef](#)]
82. Toghraie, D.; Chaharsoghi, V.; Afrand, M. Measurement of thermal conductivity of ZnO–TiO₂/EG hybrid nanofluid. *J. Therm. Anal. Calorim.* **2016**, *125*, 527–535. [[CrossRef](#)]
83. Bhanvase, B.; Kamath, S.; Patil, U.; Patil, H.; Pandit, A.; Sonawane, S. Intensification of heat transfer using PANI nanoparticles and PANI-CuO nanocomposite based nanofluids. *Chem. Eng. Process.* **2016**, *104*, 172–180. [[CrossRef](#)]
84. Asadi, A.; Alarif, I.; Foong, L. An experimental study on characterization, stability and dynamic viscosity of CuO-TiO₂/water hybrid nanofluid. *J. Mol. Liq.* **2020**, *307*, 112987. [[CrossRef](#)]
85. Chen, Z.; Shahsavari, A.; Al-Rashed, A.; Afrand, M. The impact of sonication and stirring durations on the thermal conductivity of alumina-liquid paraffin nanofluid: An experimental assessment. *Powder Technol.* **2020**, *360*, 1134–1142. [[CrossRef](#)]
86. Asadi, A.; Alarif, I.; Ali, V.; Nguyen, H. An experimental investigation on the effects of ultrasonication time on stability and thermal conductivity of MWCNT/water nanofluid: Finding the optimum ultrasonication time. *Ultrason. Sonochem.* **2019**, *58*, 104639. [[CrossRef](#)]
87. Gulzar, O.; Qayoum, A.; Gupta, R. Experimental study on stability and rheological behavior of hybrid Al₂O₃–TiO₂ Therminol-55 nanofluids for concentrating solar collectors. *Powder Technol.* **2019**, *352*, 436–444. [[CrossRef](#)]
88. Alarif, I.; Alkhouh, A.; Ali, V.; Nguyen, H.; Asadi, A. On the rheological properties of MWCNT-TiO₂/oil hybrid nanofluid: An experimental investigation on the effects of shear rate, temperature, and solid concentration of nanoparticles. *Powder Technol.* **2019**, *355*, 157–162. [[CrossRef](#)]
89. Akram, N.; Sadri, R.; Kazi, S.N.; Ahmed, S.M.; Zubir, M.N.M.; Ridha, M.; Soudagar, M.; Ahmed, W.; Arzpeyma, M.; Tong, G.B. An experimental investigation on the performance of a flat-plate solar collector using eco-friendly treated graphene nanoplatelets–water nanofluids. *J. Therm. Anal. Calorim.* **2019**, *138*, 609–621. [[CrossRef](#)]
90. Sharafeldin, M.; Grof, G. Efficiency of evacuated tube solar collector using WO₃/Water nanofluid. *Renew. Energy* **2019**, *134*, 453–460. [[CrossRef](#)]
91. Chen, W.; Zou, C.; Li, X. Application of large-scale prepared MWCNTs nanofluids in solar energy system as volumetric solar absorber. *Sol. Energy Mater. Sol. Cells* **2019**, *200*, 109931. [[CrossRef](#)]
92. Ali, N.; Teixeira, J.; Addali, A. Aluminum nanofluids stability: A comparison between the conventional two-step fabrication approach and the controlled sonication bath temperature method. *J. Nanomater.* **2019**, *2019*, 3930572. [[CrossRef](#)]
93. Mahbulbul, I.; Elcioglu, E.; Amalina, M.; Saidur, R. Stability, thermophysical properties and performance assessment of alumina–water nanofluid with emphasis on ultrasonication and storage period. *Powder Technol.* **2019**, *345*, 668–675. [[CrossRef](#)]
94. Mahyari, A.; Karimipour, A.; Afrand, M. Effects of dispersed added Graphene Oxide-Silicon Carbide nanoparticles to present a statistical formulation for the mixture thermal properties. *Phys. A Stat. Mech. Its Appl.* **2019**, *521*, 98–112. [[CrossRef](#)]
95. Chen, W.; Zou, C.; Li, X.; Liang, H. Application of recoverable carbon nanotube nanofluids in solar desalination system: An experimental investigation. *Desalination* **2019**, *451*, 92–101. [[CrossRef](#)]
96. Okonkwo, E.; Wole-Osho, I.; Kavaz, D.; Abid, M. Comparison of experimental and theoretical methods of obtaining the thermal properties of alumina/iron mono and hybrid nanofluids. *J. Mol. Liq.* **2019**, *292*, 111377. [[CrossRef](#)]
97. Teruel, M.; Aguilar, T.; Martínez-Merino, P.; Carrillo-Berdugo, I.; Gallardo-Bernal, J.J.; Gómez-Villarejo, R.; Alcántara, R.; Fernández-Lorenzo, C.; Navas, J. 2D MoSe₂-based nanofluids prepared by liquid phase exfoliation for heat transfer applications in concentrating solar power. *Sol. Energy Mater. Sol. Cells* **2019**, *200*, 109972. [[CrossRef](#)]
98. Li, Z.; Asadi, S.; Karimipour, A.; Abdollahi, A.; Tlili, I. Experimental study of temperature and mass fraction effects on thermal conductivity and dynamic viscosity of SiO₂-oleic acid/ liquid paraffin nanofluid. *Int. Commun. Heat Mass Transf.* **2020**, *110*, 104436. [[CrossRef](#)]
99. Geng, Y.; Al-Rashed, A.; Mahmoudi, B.; Alsagri, A.; Shahsavari, A.; Alebizadehsardari, P. Characterization of the nanoparticles, the stability analysis and the evaluation of a new hybrid nano-oil thermal conductivity. *J. Therm. Anal. Calorim.* **2020**, *139*, 1553–1564. [[CrossRef](#)]

100. Li, Y.; Kalbasi, R.; Nguyen, Q.; Afrand, M. Effects of sonication duration and nanoparticles concentration on thermal conductivity of silica-ethylene glycol nanofluid under different temperatures: An experimental study. *Powder Technol.* **2020**, *367*, 464–473. [[CrossRef](#)]
101. Bhattad, A.; Sarkar, J.; Ghosh, P. Experimentation on effect of particle ratio on hydrothermal performance of plate heat exchanger using hybrid nanofluid. *Appl. Therm. Eng.* **2019**, *162*, 114309. [[CrossRef](#)]
102. Yang, L.; Ji, W.; Mao, M.; Huang, J. An updated review on the properties, fabrication and application of hybrid-nanofluids along with their environmental effects. *J. Clean. Prod.* **2020**, *257*, 120408. [[CrossRef](#)]
103. Sezer, N.; Atieh, M.A.; Koç, M. A comprehensive review on synthesis, stability, thermophysical properties, and characterization of nanofluids. *Powder Technol.* **2019**, *344*, 404–431. [[CrossRef](#)]
104. Asadi, A.; Pourfattah, F.; Szilágyi, I.; Afrand, M.; Żyła, G.; Ahn, H.; Wongwises, N.H.; Arabkoohsar, A.; Mahian, O. Effect of sonication characteristics on stability, thermophysical properties, and heat transfer of nanofluids: A comprehensive review. *Ultrason. Sonochem.* **2019**, *58*, 104701. [[CrossRef](#)]
105. Lu, Y.; Lu, X.; Mayers, B.; Herricks, T.; Xia, Y. Synthesis and characterization of magnetic Co nanoparticles: A comparison study of three different capping surfactants. *J. Solid State Chem.* **2008**, *181*, 1530–1538. [[CrossRef](#)]
106. Saeedinia, M.; Akhavan-Behabadi, M.; Razi, P. Thermal and rheological characteristics of CuO-Base oil nanofluidflow inside a circular tube. *Int. Commun. Heat Mass Tran.* **2012**, *39*, 152–159. [[CrossRef](#)]
107. Khan, A.; Arasu, A. A review of influence of nanoparticle synthesis and geometrical parameters on thermophysical properties and stability of nanofluids. *Therm. Sci. Eng. Prog.* **2019**, *11*, 334–364. [[CrossRef](#)]
108. Singh, S. Review on the stability of the nanofluids. In *Pipeline Engineering*; Rushd, S., Ismail, M.A., Eds.; IntechOpen: London, UK, 2022. [[CrossRef](#)]
109. Safiei, W.; Rahman, M.; Yusoff, A.; Radin, M. Preparation, stability and wettability of nanofluid: A review. *J. Mech. Eng. Sci.* **2020**, *14*, 7244–7257. [[CrossRef](#)]
110. Amin, A.; Hamzah, W.; Oumer, A. Thermal conductivity and dynamic viscosity of mono and hybrid organic- and synthetic-based nanofluids: A critical review. *Nanotechnol. Rev.* **2021**, *10*, 1624–1661. [[CrossRef](#)]
111. Malika, M.; Sonawane, S. Effect of nanoparticle mixed ratio on stability and thermo-physical properties of CuO-ZnO/water-based hybrid nanofluid. *J. Indian Chem. Soc.* **2020**, *97*, 414–419.
112. Sahoo, R.; Kumar, V. Comparative analysis of Viscosity and Thermal Conductivity for Al₂O₃/CuO Hybrid Nanofluid in Binary Base Fluids. *Nanotechnol. Mater. Sci.* **2019**, *6*, 34–42.
113. Ramadhan, A.; Azmi, W.; Mamat, R.; Hamid, K.; Norsakinah, S. Investigation on stability of tri-hybrid nanofluids in water-ethylene glycol mixture. *IOP Conf. Ser. Mater. Sci. Eng.* **2019**, *469*, 012068. [[CrossRef](#)]
114. Afshari, F.; Manay, E.; Rahimpour, S.; Sahin, B.; Muratçobanoğlu, B.; Teimuri-Mofrad, R. A review study on factors affecting the stability of nanofluids. *Heat Transf. Res.* **2022**, *53*, 77–91. [[CrossRef](#)]
115. Arora, N.; Gupta, M. Stability Evaluation and Enhancement Methods in Nanofluids: A Review. *AIP Conf. Proc.* **2021**, *2341*, 040022. [[CrossRef](#)]
116. Wcislik, S. Efficient stabilization of mono and hybrid nanofluids. *Energies* **2020**, *13*, 3793. [[CrossRef](#)]
117. Bumataria, R.; Chavda, N.; Panchal, H. Current research aspects in mono and hybrid nanofluid based heat pipe technologies. *Heliyon* **2019**, *5*, e01627. [[CrossRef](#)] [[PubMed](#)]
118. Ali, A.; Salam, B. A review on nanofluid: Preparation, stability, thermophysical properties, heat transfer characteristics and application. *SN Appl. Sci.* **2020**, *2*, 1636. [[CrossRef](#)]
119. Xu, Q.; Liu, L.; Feng, J.; Qiao, L.; Yu, C.; Shi, W.; Ding, C.; Zang, Y.; Chang, C.; Xiong, Y.; et al. A comparative investigation on the effect of different nanofluids on the thermal performance of two-phase closed thermosiphon. *Int. J. Heat Mass Transf.* **2020**, *149*, 119189. [[CrossRef](#)]
120. Said, Z.; Abdelkareem, M.; Rezk, H.; Nassef, A.; Atwany, H. Stability, thermophysical and electrical properties of synthesized carbon nanofiber and reduced-graphene oxidebased nanofluids and their hybrid along with fuzzy modeling approach. *Powder Technol.* **2020**, *364*, 795–809. [[CrossRef](#)]
121. Muthoka, M.; Xuelai, Z.; Xiaoafeng, X. Experimental investigation on supercooling, thermal conductivity and stability of nanofluid based composite phase change material. *J. Energy Storage* **2018**, *17*, 47–55.
122. Said, Z.; Allagui, A.; Abdelkareem, M.; Alawadhi, H.; Elsaid, K. Acid functionalized carbon nanofibers for high stability, thermoelectrical and electrochemical properties of nanofluids. *J. Colloid Interface Sci.* **2018**, *18*, 30190–30195. [[CrossRef](#)]
123. Alawi, O.; Mallah, A.; Kazi, S.; Sidik, N.; Najafi, G. Thermophysical properties and stability of carbon nanostructures and metallic oxides nanofluids. *J. Therm. Anal. Calor.* **2019**, *135*, 1545–1562. [[CrossRef](#)]
124. Akbari, A.; Saidi, M. Experimental investigation of nanofluid stability on thermal performance and flow regimes in pulsating heat pipe. *J. Therm. Anal. Calor.* **2019**, *135*, 1835–1847. [[CrossRef](#)]
125. Boroomandpour, A.; Toghraie, D.; Hashemian, M. A comprehensive experimental investigation of thermal conductivity of a ternary hybrid nanofluid containing MWCNTs- titania zinc oxide/water water ethylene (80:20) as well as binary and mono nanofluids. *Synth. Met.* **2020**, *268*, 116501. [[CrossRef](#)]
126. Uysal, A. Investigation of flank wear in MQL milling of ferritic stainless steel by using nano graphene reinforced vegetable cutting fluid. *Ind. Lubr. Tribol.* **2016**, *68*, 446–451. [[CrossRef](#)]

127. Al-Waeli, A.H.A.; Chaichan, M.T.; Kazem, H.A.; Sopian, K. Evaluation and analysis of nanofluid and surfactant impact on photovoltaic-thermal systems. *Case Stud. Therm. Eng.* **2019**, *13*, 100392. [[CrossRef](#)]
128. Cacua, K.; Ordoñez, F.; Zapata, C.; Herrera, B.; Pabón, E.; Buitrago-Sierra, R. Surfactant concentration and pH effects on the zeta potential values of alumina nanofluids to inspect stability. *Colloids Surf. A Physicochem. Eng. Asp.* **2019**, *583*, 123960. [[CrossRef](#)]
129. Kazemi, I.; Sefid, M.; Afrand, M. A novel comparative experimental study on rheological behavior of mono & hybrid nanofluids concerned graphene and silica nano-powders: Characterization, stability and viscosity measurements. *Powder Technol.* **2020**, *366*, 216–229.
130. Xian, H.; Sidik, N.; Saidur, R. Impact of different surfactants and ultrasonication time on the Stability and thermophysical properties of hybrid nanofluids. *Int. Commun. Heat Mass Transf.* **2020**, *110*, 104389. [[CrossRef](#)]
131. Almanassra, I.; Manasrah, A.; Al-Mubaiyedh, U.; Al-Ansari, T.; Malaibari, Z.; Atieh, M. An experimental study on stability and thermal conductivity of water/CNTs nanofluids using different surfactants: A comparison study. *J. Mol. Liq.* **2019**, *19*, 30396–30397. [[CrossRef](#)]
132. Cacua, K.; Buitrago-Sierra, R.; Pabon, E.; Gallego, A.; Zapata, C.; Herrera, B. Nanofluids stability effect on a thermosyphon thermal performance. *Int. J. Therm. Sci.* **2020**, *153*, 106347. [[CrossRef](#)]
133. Ouikhalfan, M.; Labihi, A.; Belaqqiz, M.; Chehouani, H.; Benhamou, B.; Sari, A.; Belfkira, A. Stability and thermal conductivity enhancement of aqueous nanofluid based on surfactant-modified TiO₂. *J. Dispers. Sci. Technol.* **2020**, *41*, 374–382. [[CrossRef](#)]
134. Siddiqui, F.; Tso, C.; Chan, K.; Fu, S.; Chao, C. On trade-off for dispersion stability and thermal transport of Cu-Al₂O₃ hybrid nanofluid for various mixing ratios. *Int. J. Heat Mass Transf.* **2019**, *132*, 1200–1216. [[CrossRef](#)]
135. Etedali, S.; Afrand, M.; Abdollahi, A. Effect of different surfactants on the pool boiling heat transfer of SiO₂/ deionized water nanofluid on a copper surface. *Int. J. Therm. Sci.* **2019**, *145*, 105977. [[CrossRef](#)]
136. Giwa, S.; Sharifpur, M.; Goodarzi, M.; Alsulami, H.; Meyer, J. Influence of base fluid, temperature, and concentration on the thermophysical properties of hybrid nanofluids of alumina–ferrofluid: Experimental data, modeling through enhanced ANN, ANFIS, and curve fitting. *J. Therm. Anal. Calorim.* **2020**, *6*, 4149–4167. [[CrossRef](#)]
137. Kazemi, I.; Sefid, M.; Afrand, M. Improving the thermal conductivity of water by adding mono & hybrid nanoadditives containing graphene and silica: A comparative experimental study. *Int. Commun. Heat Mass Transf.* **2020**, *116*, 104648.
138. Gallego, A.; Cacua, K.; Herrera, B.; Cabaleiro, D.; Piñeiro, M.; Lugo, L. Experimental evaluation of the effect in the stability and thermophysical properties of water-Al₂O₃ based nanofluids using SDBS as dispersant agent. *Adv. Powder Technol.* **2020**, *31*, 560–570. [[CrossRef](#)]
139. Shah, S.N.A.; Shahabuddin, S.; Sabri, M.F.M.; Salleh, M.F.M.; Ali, M.A.; Hayat, N.; Sidik, N.; Smykano, M.; Saidur, R. Experimental investigation on stability, thermal conductivity and rheological properties of rGO/ethylene glycol based nanofluids. *Int. J. Heat Mass Transf.* **2020**, *150*, 118981. [[CrossRef](#)]
140. Ilyas, S.; Ridha, S.; Kareem, F. Dispersion stability and surface tension of SDS Stabilized saline nanofluids with graphene nanoplatelets. *Colloids Surf. A Physicochem. Eng. Asp.* **2020**, *592*, 124584. [[CrossRef](#)]
141. Wu, S.; Ortiz, C. Experimental investigation of the effect of magnetic field on vapour absorption with LiBr-H₂O nanofluid. *Energy* **2020**, *193*, 116640. [[CrossRef](#)]
142. Xiao, X.; Jia, H.; Wen, D.; Zhao, X. Thermal performance analysis of a solar energy storage unit encapsulated with HITEC salt/copper foam/nanoparticles composite. *Energy* **2020**, *192*, 116593. [[CrossRef](#)]
143. Lee, J.; Kang, Y. CO₂ absorption enhancement by Al₂O₃ nanoparticles in NaCl aqueous solution. *Energy* **2020**, *53*, 206–211. [[CrossRef](#)]
144. Vajjha, R.; Das, D. Experimental determination of thermal conductivity of three nanofluids and development of new correlations. *Int. J. Heat Mass Transf.* **2009**, *52*, 4675–4682. [[CrossRef](#)]
145. Zhou, Y.; Zheng, S. Multi-level uncertainty optimisation on phase change materials integrated renewable systems with hybrid ventilations and active cooling. *Energy* **2020**, *202*, 117747. [[CrossRef](#)]
146. Khodadadi, H.; Aghakhani, S.; Majd, H.; Kalbasi, R.; Wongwises, S.; Afrand, M. A comprehensive review on rheological behavior of mono and hybrid nanofluids: Effective parameters and predictive correlations. *Int. J. Heat Mass Transf.* **2018**, *127*, 997–1012. [[CrossRef](#)]
147. Sajid, M.; Ali, H. Thermal conductivity of hybrid nanofluids: A critical review. *Int. J. Heat Mass Transf.* **2018**, *126*, 211–234. [[CrossRef](#)]
148. Askari, S.; Lotfi, R.; Rashidi, A.; Koolivand, H.; Koolivand-Salooki, M. Rheological and thermophysical properties of ultra-stable kerosene-based Fe₃O₄/Graphene nanofluids for energy conservation. *Energy Convers. Manag.* **2016**, *128*, 134–144. [[CrossRef](#)]
149. Ho, C.; Huang, J.; Tsai, P.; Yang, Y. Preparation and properties of hybrid water-based suspension of Al₂O₃ nanoparticles and MEPCM particles as functional forced convection fluid. *Int. Commun. Heat Mass Transf.* **2010**, *37*, 490–494. [[CrossRef](#)]
150. Baghbanzadeh, M.; Rashidi, A.; Rashtchian, D.; Lotfi, R.; Amrollahi, A. Synthesis of spherical silica/multiwall carbon nanotubes hybrid nanostructures and investigation of thermal conductivity of related nanofluids. *Thermochim. Acta* **2012**, *549*, 87–94. [[CrossRef](#)]
151. Labib, M.; Nine, M.; Afrianto, H.; Chung, H.; Jeong, H. Numerical investigation on effect of base fluids and hybrid nanofluid in forced convective heat transfer. *Int. J. Therm. Sci.* **2013**, *71*, 163–171. [[CrossRef](#)]
152. Nguyen, C.; Desgranges, F.; Galanis, N.; Roy, G.; Mare, T.; Boucher, S.; Mintsa, H. Viscosity data for Al₂O₃-water nanofluid-hysteresis: Is heat transfer enhancement using nanofluids reliable? *Int. J. Therm. Sci.* **2008**, *47*, 103–111. [[CrossRef](#)]

153. Kishore, P.; Sireesha, V.; Harsha, V.; Rao, V.; Solomon, A. Preparation, characterization and thermo-physical properties of Cu-graphene nanoplatelets hybrid nanofluids. *Mater. Today Proc.* **2020**, *27*, 610–614. [[CrossRef](#)]
154. Yu, W.; Xie, H.; Chen, L.; Li, Y. Investigation of thermal conductivity and viscosity of ethylene glycol based ZnO nanofluid. *Thermochim. Acta* **2009**, *491*, 92–96. [[CrossRef](#)]
155. Esfe, M.; Afrand, M.; Yan, W.; Yarmand, H.; Toghraie, D.; Dahari, M. Effects of temperature; concentration on rheological behavior of MWCNTs/SiO₂ (20-80)-SAE40 hybrid nano-lubricant. *Int. Commun. Heat Mass Transf.* **2016**, *76*, 133–138. [[CrossRef](#)]
156. Dardan, E.; Afrand, M.; Meghdadi-Isfahani, A. Effect of suspending hybrid nano-additives on rheological behavior of engine oil and pumping power. *Appl. Therm. Eng.* **2016**, *109*, 524–534. [[CrossRef](#)]
157. Soltani, O.; Akbari, M. Effects of temperature and particles concentration on the dynamic viscosity of MgO-MWCNT/ethylene glycol hybrid nanofluid: Experimental study. *Phys. E Low Dimens. Syst. Nanostructures* **2016**, *84*, 564–570. [[CrossRef](#)]
158. Esfe, M.; Raki, H.; Emami, M.; Afrand, M. Viscosity and rheological properties of antifreeze based nanofluid containing hybrid nano-powders of MWCNTs and TiO₂ under different temperature conditions. *Powder Technol.* **2019**, *342*, 808–816. [[CrossRef](#)]
159. Asadi, M.; Asadi, A. Dynamic viscosity of MWCNT/ZnO-engine oil hybrid nanofluid: An experimental investigation and new correlation in different temperatures and solid concentrations. *Int. Commun. Heat Mass Transf.* **2016**, *76*, 41–45. [[CrossRef](#)]
160. Esfe, M.; Arani, A.; Rezaei, M.; Yan, W.; Karimipour, A. Experimental determination of thermal conductivity and dynamic viscosity of Ag-MgO/water hybrid nanofluid. *Int. Commun. Heat Mass Transf.* **2015**, *66*, 189–195. [[CrossRef](#)]
161. Yarmand, H.; Gharekhani, S.; Ahmadi, G.; Shirazi, S.; Baradaran, S.; Montazer, E.; Zubir, M.; Alehashem, M.; Kazi, S.; Dahari, M. Graphene nanoplatelets-silver hybrid nanofluids for enhanced heat transfer. *Energy Convers. Manag.* **2015**, *100*, 419–428. [[CrossRef](#)]
162. Sundar, L.; Ramana, E.; Graça, M.; Singh, M.; Sousa, A. Nanodiamond-Fe₃O₄ nanofluids: Preparation and measurement of viscosity, electrical and thermal conductivities. *Int. Commun. Heat Mass Transf.* **2016**, *73*, 62–74. [[CrossRef](#)]
163. Afrand, M.; Najafabadi, K.; Akbari, M. Effects of temperature and solid volume fraction on viscosity of SiO₂-MWCNTs/SAE40 hybrid nanofluid as a coolant and lubricant in heat engines. *Appl. Therm. Eng.* **2016**, *102*, 45–54. [[CrossRef](#)]
164. Esfe, M.; Afrand, M.; Rostamian, S.; Toghraie, D. Examination of rheological behavior of MWCNTs/ZnO-SAE40 hybrid nano-lubricants under various temperatures and solid volume fractions. *Exp. Therm. Fluid Sci.* **2017**, *80*, 384–390. [[CrossRef](#)]
165. Sheikholeslami, M.; Shamlooei, M. Magnetic source influence on nanofluid flow in porous medium considering shape factor effect. *Phys. Lett. A* **2017**, *381*, 3071–3078. [[CrossRef](#)]
166. Asadi, A.; Asadi, M.; Rezaei, M.; Siahmargoi, M.; Asadi, F. The effect of temperature and solid concentration on dynamic viscosity of MWCNT/MgO (20–80)-SAE50 hybrid nano-lubricant and proposing a new correlation: An experimental study. *Int. Commun. Heat Mass Transf.* **2016**, *78*, 48–53. [[CrossRef](#)]
167. Riahi, A.; Khamlich, S.; Balghouthi, M.; Khamliche, T.; Doyle, T.; Dimassi, W.; Guizani, A.; Maaza, M. Study of thermal conductivity of synthesized Al₂O₃-water nanofluid by pulsed laser ablation in liquid. *J. Mol. Liq.* **2020**, *304*, 112694. [[CrossRef](#)]
168. Hamze, S.; Berrada, N.; Cabaleiro, D.; Desforgues, A.; Ghanbaja, J.; Gleize, J.; Bégin, D.; Michaux, F.; Maré, T.; Vigolo, B.; et al. Few-layer graphene-based nanofluids with enhanced thermal conductivity. *Nanomaterials* **2020**, *10*, 1258. [[CrossRef](#)] [[PubMed](#)]
169. Hamze, S.; Cabaleiro, D.; Maré, T.; Vigolo, B.; Estellé, P. Shear flow behavior and dynamic viscosity of few-layer graphene nanofluids based on propylene glycol-water mixture. *J. Mol. Liq.* **2020**, *316*, 113875. [[CrossRef](#)]
170. Charab, A.; Movahedirad, S.; Norouzbeigi, R. Thermal conductivity of Al₂O₃ + TiO₂/water nanofluid: Model development and experimental validation. *Appl. Therm. Eng.* **2017**, *119*, 42–51. [[CrossRef](#)]
171. Nine, M.; Batmunkh, M.; Kim, J.; Chung, H.; Jeong, H. Investigation of Al₂O₃-MWCNTs hybrid dispersion in water and their thermal characterization. *J. Nanosci. Nanotechnol.* **2012**, *12*, 4553–4559. [[CrossRef](#)] [[PubMed](#)]
172. Shahsavar, A.; Salimpour, M.; Saghafian, M.; Shafii, M. An experimental study on the effect of ultrasonication on thermal conductivity of ferrofluid loaded with carbon nanotubes. *Thermochim. Acta* **2015**, *617*, 102–110. [[CrossRef](#)]
173. Farbod, M.; Ahangarpour, A. Improved thermal conductivity of Ag decorated carbon nanotubes water based nanofluids. *Phys. Lett. Sect. A* **2016**, *380*, 4044–4048. [[CrossRef](#)]
174. Harandi, S.; Karimipour, A.; Afrand, M.; Akbari, M.; D’Orazio, A. An experimental study on thermal conductivity of F-MWCNTs-Fe₃O₄/EG hybrid nanofluid: Effects of temperature and concentration. *Int. Commun. Heat Mass Transf.* **2016**, *76*, 171–177. [[CrossRef](#)]
175. Yarmand, H.; Gharekhani, S.; Shirazi, S.; Amiri, A.; Montazer, E.; Arzani, H.; Sadri, R.; Dahari, M.; Kazi, S. Nanofluid based on activated hybrid of biomass carbon/graphene oxide: Synthesis, thermo-physical and electrical properties. *Int. Commun. Heat Mass Transf.* **2016**, *72*, 10–15. [[CrossRef](#)]
176. Chougule, S.; Sahu, S. Model of heat conduction in hybrid nanofluid. In Proceedings of the 2013 IEEE International Conference ON Emerging Trends in Computing, Communication and Nanotechnology (ICECCN), Tirunelveli, India, 25–26 March 2013; pp. 337–341.
177. Takabi, B.; Salehi, S. Augmentation of the heat transfer performance of a sinusoidal corrugated enclosure by employing hybrid nanofluid. *Adv. Mech. Eng.* **2014**, *2014*, 147059. [[CrossRef](#)]
178. Esfe, M.; Saedodin, S.; Biglari, M.; Rostamian, H. Experimental investigation of thermal conductivity of CNTs-Al₂O₃/water: A statistical approach. *Int. Commun. Heat Mass Transf.* **2015**, *69*, 29–33. [[CrossRef](#)]

179. Esfe, M.; Wongwises, S.; Naderi, A.; Asadi, A.; Safaei, M.; Rostamian, H.; Dahari, M.; Karimipour, A. Thermal conductivity of Cu/TiO₂-water/EG hybrid nanofluid: Experimental data and modeling using artificial neural network and correlation. *Int. Commun. Heat Mass Transf.* **2015**, *66*, 100–104. [[CrossRef](#)]
180. Esfe, M.; Yan, W.; Akbari, M.; Karimipour, A.; Hassani, M. Experimental study on thermal conductivity of DWCNT-ZnO/water-EG nanofluids. *Int. Commun. Heat Mass Transf.* **2015**, *68*, 248–251. [[CrossRef](#)]
181. Afrand, M. Experimental study on thermal conductivity of ethylene glycol containing hybrid nano-additives and development of a new correlation. *Appl. Therm. Eng.* **2017**, *110*, 1111–1119. [[CrossRef](#)]
182. Vafaei, M.; Afrand, M.; Sina, N.; Kalbasi, R.; Sourani, F.; Teimouri, H. Evaluation of thermal conductivity of MgO-MWCNTs/EG hybrid nanofluids based on experimental data by selecting optimal artificial neural networks. *Phys. E Low Dimens. Syst. Nanostructures* **2017**, *85*, 90–96. [[CrossRef](#)]
183. Esfe, M.; Alirezaie, A.; Rejvani, M. An applicable study on the thermal conductivity of SWCNT-MgO hybrid nanofluid and price-performance analysis for energy management. *Appl. Therm. Eng.* **2017**, *111*, 1202–1210. [[CrossRef](#)]
184. Esfe, M.; Behbahani, P.; Arani, A.; Sarlak, M. Thermal conductivity enhancement of SiO₂-MWCNT (85:15%)-EG hybrid nanofluids: ANN designing, experimental investigation, cost performance and sensitivity analysis. *J. Therm. Anal. Calorim.* **2017**, *128*, 249–258. [[CrossRef](#)]
185. Esfe, M.; Esfandeh, S.; Rejvani, M. Modeling of thermal conductivity of MWCNT-SiO₂ (30:70%)/EG hybrid nanofluid, sensitivity analyzing and cost performance for industrial applications. *J. Therm. Anal. Calorim.* **2018**, *131*, 1437–1447. [[CrossRef](#)]
186. Esfe, H.M.; Arani, A.A.A.; Badi, S.R.; Rejvani, M. ANN modeling, cost performance and sensitivity analyzing of thermal conductivity of DWCNT-SiO₂/EG hybrid nanofluid for higher heat transfer: An experimental study. *J. Therm. Anal. Calorim.* **2017**, *131*, 2381–2393. [[CrossRef](#)]
187. Esfe, M.; Rejvani, M.; Karimpour, R.; Arani, A. Estimation of thermal conductivity of ethylene glycol-based nanofluid with hybrid suspensions of SWCNT-Al₂O₃ nanoparticles by correlation and ANN methods using experimental data. *J. Therm. Anal. Calorim.* **2017**, *128*, 1359–1371. [[CrossRef](#)]
188. Rostamian, S.; Biglari, M.; Saedodin, S.; Esfe, M. An inspection of thermal conductivity of CuO-SWCNTs hybrid nanofluid versus temperature and concentration using experimental data, ANN modeling and new correlation. *J. Mol. Liq.* **2017**, *231*, 364–369. [[CrossRef](#)]
189. Zadkhast, M.; Toghraie, D.; Karimipour, A. Developing a new correlation to estimate the thermal conductivity of MWCNT-CuO/water hybrid nanofluid via an experimental investigation. *J. Therm. Anal. Calorim.* **2017**, *129*, 859–867. [[CrossRef](#)]
190. Elias, M.; Shahrul, I.; Mahbulul, I.; Saidur, R.; Rahim, N. Effect of different nanoparticle shapes on shell and tube heat exchanger using different baffle angles and operated with nanofluid. *Int. J. Heat Mass Transf.* **2014**, *70*, 289–297. [[CrossRef](#)]
191. Vajjha, R.; Das, D.K. A review and analysis on influence of temperature and concentration of nanofluids on thermophysical properties, heat transfer and pumping power. *Int. J. Heat Mass Transf.* **2012**, *55*, 4063–4078. [[CrossRef](#)]
192. Huminic, G.; Huminic, A. Application of nanofluids in heat exchangers: A review. *Renew. Sustain. Energy Rev.* **2012**, *16*, 5625–5638. [[CrossRef](#)]
193. Huminic, G.; Huminic, A. Hybrid nanofluids for heat transfer applications—A state-of-the-art review. *Int. J. Heat Mass Transf.* **2018**, *125*, 82–103. [[CrossRef](#)]
194. Anoop, K.; Cox, J.; Sadr, R. Thermal evaluation of nanofluids in heat exchangers. *Int. Commun. Heat Mass Transf.* **2013**, *49*, 5–9. [[CrossRef](#)]
195. Kumar, V.; Tiwari, A.; Ghosh, S. Application of nanofluids in plate heat exchanger: A review. *Energy Convers. Manag.* **2015**, *105*, 1017–1036. [[CrossRef](#)]
196. Azmi, W.; Hamid, K.; Usri, N.; Mamat, R.; Sharma, K. Heat transfer augmentation of ethylene glycol: Water nanofluids and applications—A review. *Int. Commun. Heat Mass Transf.* **2016**, *75*, 13–23. [[CrossRef](#)]
197. Minea, A. Challenges in hybrid nanofluids behavior in turbulent flow: Recent research and numerical comparison. *Renew. Sustain. Energy Rev.* **2017**, *71*, 426–434. [[CrossRef](#)]
198. Elmaaty, T.A.; Kabeel, A.; Mahgoub, M. Corrugated plate heat exchanger review. *Renew. Sustain. Energy Rev.* **2017**, *70*, 852–860. [[CrossRef](#)]
199. Zheng, D.; Wang, J.; Pang, Y.; Chen, Z.; Sunden, B. Heat transfer performance and friction factor of various nanofluids in a double-tube counter flow heat exchanger. *Therm. Sci.* **2020**, *24*, 3601–3612. [[CrossRef](#)]
200. Zheng, D.; Wang, J.; Chen, Z.; Baleta, J.; Sundén, B. Performance analysis of a plate heat exchanger using various nanofluids. *Int. J. Heat Mass Transf.* **2020**, *158*, 119993. [[CrossRef](#)]
201. Babu, C.R.; Kumar, P.; Roy, S.; Ganesan, R. A comprehensive review on compound heat transfer enhancement using passive techniques in a heat exchanger. *Mater. Today Proc.* **2021**, *54*, 428–436.
202. Bakthavatchalam, B.; Habib, K.; Saidur, R.; Saha, B.; Irshad, K. Comprehensive study on nanofluid and ionanofluid for heat transfer enhancement: A review on current and future perspective. *J. Mol. Liq.* **2020**, *305*, 112787. [[CrossRef](#)]
203. Pandey, S.; Nema, V. Experimental analysis of heat transfer and friction factor of nanofluid as a coolant in a corrugated plate heat exchanger. *Exp. Therm. Fluid Sci.* **2012**, *38*, 248–256. [[CrossRef](#)]
204. Tiwari, A.; Ghosh, P.; Sarkar, J. Performance comparison of the plate heat exchanger using different nanofluids. *Exp. Therm. Fluid Sci.* **2013**, *49*, 141–151. [[CrossRef](#)]

205. Tiwari, A.; Ghosh, P.; Sarkar, J. Particle concentration levels of various nanofluids in plate heat exchanger for best performance. *Int. J. Heat Mass Transf.* **2015**, *89*, 1110–1118. [[CrossRef](#)]
206. Barzegarian, R.; Moraveji, M.; Aloueyan, A. Experimental investigation on heat transfer characteristics and pressure drop of BPHE (brazed plate heat exchanger) using TiO₂-water nanofluid. *Exp. Therm. Fluid Sci.* **2016**, *74*, 11–18. [[CrossRef](#)]
207. Tabari, Z.T.; Heris, S.Z.; Kahani, M. The study on application of TiO₂/water nanofluid in plate heat exchanger of milk pasteurization industries. *Renew. Sustain. Energy Rev.* **2016**, *58*, 1318–1326. [[CrossRef](#)]
208. Prashant, G.S.; Sarao, T. Experimental analysis of heat transfer and friction factor in plate heat exchanger with different orientations using Al₂O₃ nanofluids. *Int. J. Eng.* **2016**, *29*, 1450–1458.
209. Huang, D.; Wu, Z.; Sunden, B. Pressure drop and convective heat transfer of Al₂O₃/water and MWCNT/water nanofluids in a chevron plate heat exchanger. *Int. J. Heat Mass Transf.* **2015**, *89*, 620–626. [[CrossRef](#)]
210. Bhattad, A.; Sarkar, J.; Ghosh, P. Hydrothermal performance of different alumina hybrid nanofluid types in plate heat exchanger. *J. Therm. Anal. Calorim.* **2020**, *139*, 3777–3787. [[CrossRef](#)]
211. Bhattad, A.; Sarkar, J.; Ghosh, P. Heat transfer characteristics of plate heat exchanger using hybrid nanofluids: Effect of nanoparticle mixture ratio. *Heat Mass Transf.* **2020**, *56*, 2457–2472. [[CrossRef](#)]
212. Bhattad, A. Experimental investigation of Al₂O₃-MgO hot hybrid nanofluid in a plate heat exchanger. *Heat Transf.* **2020**, *49*, 2344–2354. [[CrossRef](#)]
213. Bhattad, A. Exergy analysis of plate heat exchanger with graphene alumina hybrid nanofluid: Experimentation. *Int. J. Exergy* **2020**, *33*, 254–262. [[CrossRef](#)]
214. Kavitha, R.; Algani, Y.; Kulkarni, K.; Gupta, M. Heat transfer enhancement in a double pipe heat exchanger with copper oxide nanofluid: An experimental study. *Mater. Today Proc.* **2021**, *56*, 3446–3449. [[CrossRef](#)]
215. Jassim, E.; Ahmed, F. Assessment of nanofluid on the performance and energy-environment interaction of Plate-Type-Heat exchanger. *Therm. Sci. Eng. Prog.* **2021**, *25*, 100988. [[CrossRef](#)]
216. Jassim, E.; Ahmed, F. Experimental assessment of Al₂O₃ and Cu nanofluids on the performance and heat leak of double pipe heat exchanger. *Heat Mass Transf.* **2020**, *56*, 1845–1858. [[CrossRef](#)]
217. Mansoury, D.; Doshmanziari, F.; Kiani, A.; Chamkha, A.; Sharifpur, M. Heat transfer and flow characteristics of Al₂O₃/water nanofluid in various heat exchangers: Experiments on counter flow. *Heat Transf. Eng.* **2019**, *41*, 220–234. [[CrossRef](#)]
218. Henein, S.; Abdel-Rehim, A. The performance response of a heat pipe evacuated tube solar collector using MgO/MWCNT hybrid nanofluid as a working fluid. *Case Stud. Therm. Eng.* **2022**, *33*, 101957. [[CrossRef](#)]
219. Heyhat, M.; Abdi, A.; Jafarizad, A. Performance evaluation and exergy analysis of a double pipe heat exchanger under air bubble injection. *Appl. Therm. Eng.* **2018**, *143*, 582–593. [[CrossRef](#)]
220. Hosseinian, A.; Isfahani, A. Experimental study of heat transfer enhancement due to the surface vibrations in a flexible double pipe heat exchanger. *Heat Mass Transf.* **2017**, *54*, 1113–1120. [[CrossRef](#)]
221. Bezaatpour, M.; Goharkhah, M. Convective heat transfer enhancement in a double pipe mini heat exchanger by magnetic field induced swirling flow. *Appl. Therm. Eng.* **2020**, *167*, 114801. [[CrossRef](#)]
222. Setareh, M.; Saffar-Avval, M.; Abdullah, A. Experimental and numerical study on heat transfer enhancement using ultrasonic vibration in a double-pipe heat exchanger. *Appl. Therm. Eng.* **2019**, *159*, 113867. [[CrossRef](#)]
223. Akbarzadeh, M.; Rashidi, S.; Keshmiri, A.; Shokri, N. The optimum position of porous insert for a double-pipe heat exchanger based on entropy generation and thermal analysis. *J. Therm. Anal.* **2020**, *139*, 411–426. [[CrossRef](#)]
224. Poongavanam, G.; Panchabikesan, K.; Murugesan, R.; Duraisamy, S.; Ramalingam, V. Experimental investigation on heat transfer and pressure drop of MWCNT-Solar glycol based nanofluids in shot peened double pipe heat exchanger. *Powder Technol.* **2019**, *345*, 815–824. [[CrossRef](#)]
225. Arya, H.; Sarafraz, M.; Pourmehrhan, O.; Arjomandi, M. Performance index improvement of a double-pipe cooler with MgO/waterethylene glycol (50:50) nano-suspension. *Propuls. Power Res.* **2020**, *9*, 75–86. [[CrossRef](#)]
226. Subramanian, R.; Kumar, A.S.; Vinayagar, K.; Muthusamy, S. Experimental analyses on heat transfer performance of TiO₂-water nanofluid in double-pipe counter-flow heat exchanger for various flow regimes. *J. Therm. Anal.* **2020**, *140*, 603–612. [[CrossRef](#)]
227. Dalkılıç, A.S.; Mercan, H.; Özçelik, G.; Wongwises, S. Optimization of the finned double-pipe heat exchanger using nanofluids as working fluids. *J. Therm. Anal.* **2021**, *143*, 859–878. [[CrossRef](#)]
228. Bahmani, M.H.; Sheikhzadeh, G.; Zarringhalam, M.; Akbari, O.A.; Alrashed, A.A.; Shabani, G.A.S.; Goodarzi, M. Investigation of turbulent heat transfer and nanofluid flow in a double pipe heat exchanger. *Adv. Powder Technol.* **2018**, *29*, 273–282. [[CrossRef](#)]
229. Bahmani, M.H.; Akbari, O.A.; Zarringhalam, M.; Shabani, G.A.S.; Goodarzi, M. Forced convection in a double tube heat exchanger using nanofluids with constant and variable thermophysical properties. *Int. J. Numer. Methods Heat Fluid Flow* **2019**, *30*, 3247–3265. [[CrossRef](#)]
230. Kristiawan, B.; Rifa, A.; Enoki, K.; Wijayanta, A.; Miyazaki, T. Enhancing the thermal performance of TiO₂/water nanofluids flowing in a helical microfin tube. *Powder Technol.* **2020**, *376*, 254–262. [[CrossRef](#)]
231. Akachi, H. Structure of a Heat Pipe. U.S. Patent 4921041; *Scientific research an academic publisher*, 1990.
232. Singh, U.; Kumar, N. Stability issues and operating limitations of nanofluid filled heat pipe: A critical review. *Mater. Today Proc.* **2023**, *in press*. [[CrossRef](#)]
233. Karthikeyan, V.K.; Ramachandran, K.; Pillai, B.C.; Solomon, A.B. Effect of nanofluids on thermal performance of closed loop pulsating heat pipe. *Exp. Therm. Fluid Sci.* **2014**, *54*, 171–178. [[CrossRef](#)]

234. Goshayeshi, H.R.; Safaei, M.R.; Goodarzi, M.; Dahari, M. Particle size and type effects on heat transfer enhancement of ferro-nanofluids in a pulsating heat pipe. *Powder Technol.* **2016**, *301*, 1218–1226. [[CrossRef](#)]
235. Li, Z. Operation analysis, response and performance evaluation of a pulsating heat pipe for low temperature heat recovery. *Energy Convers. Manag.* **2020**, *222*, 113230. [[CrossRef](#)]
236. Kim, H.-T.; Bang, K.-H. Heat transfer enhancement of nanofluids in a pulsating heat pipe for heat dissipation of led lighting. *J. Korean Soc. Manuf. Process Eng.* **2014**, *38*, 1200–1205. [[CrossRef](#)]
237. Kang, S.W.; Wang, Y.C.; Liu, Y.C.; Lo, H.M. Visualization and thermal resistance measurements for a magnetic nanofluid pulsating heat pipe. *Appl. Therm. Eng.* **2017**, *126*, 1044–1050. [[CrossRef](#)]
238. Wu, H. Thermal performance comparison of oscillating heat pipes with SiO₂/water and Al₂O₃/water nanofluids. *Int. J. Therm. Sci.* **2011**, *50*, 1954–1962.
239. Goshayeshi, H.R.; Izadi, F.; Bashirnezhad, K. Comparison of heat transfer performance on closed pulsating heat pipe for Fe₃O₄ and γ-Fe₂O₃ for achieving an empirical correlation. *Phys. E Low Dimens. Syst. Nanostruct.* **2017**, *89*, 43–49. [[CrossRef](#)]
240. Xu, R.; Wang, R.; Li, Y. Effect of C60 nanofluid on the thermal performance of a flat-plate pulsating heat pipe. *Int. J. Heat Mass Transf.* **2016**, *100*, 892–898.
241. Xue, Y.; Qi, H.; Cai, W. Experimental study on heat transfer performance of pulsating heat pipes with hybrid working fluids. *Int. J. Heat Mass Transf.* **2020**, *157*, 119727. [[CrossRef](#)]
242. Zufar, G.P.; Kumar, H.M.; Ng, K.C. Numerical and experimental investigations of hybrid nanofluids on pulsating heat pipe performance. *Int. J. Heat Mass Transf.* **2020**, *146*, 118887. [[CrossRef](#)]
243. Khodami, R.; Nejad, A.A.; Khabbaz, M.R.A. Experimental investigation of energy and exergy efficiency of a pulsating heat pipe for chimney heat recovery. *Sustain. Energy Technol. Assess.* **2016**, *16*, 11–17. [[CrossRef](#)]
244. Jahani, M.M.; Shafii, M.B.; Shiee, Z. Promising technology for electronic cooling: Nanofluidic micro pulsating heat pipes. *J. Electron. Packag.* **2013**, *135*, 021005. [[CrossRef](#)]
245. Zhang, M.; Han, W.; Guo, X. Enhancement of heat transport in oscillating heat pipe with ternary fluid. *Int. J. Heat Mass Transf.* **2015**, *87*, 258–264.
246. Babar, H.; Ali, H. Towards hybrid nanofluids: Preparation, thermophysical properties, applications, and challenges. *J. Mol. Liq.* **2019**, *281*, 598–633. [[CrossRef](#)]
247. Selvakumar, P.; Suresh, S. Use of Al₂O₃-Cu/water hybrid nanofluid in an electronic heat sink. *IEEE Trans. Compon. Packag. Manuf. Technol.* **2012**, *2*, 1600–1607. [[CrossRef](#)]
248. Ahammed, N.; Asirvatham, L.; Wongwises, S. Entropy generation analysis of graphene–alumina hybrid nanofluid in multiport mini channel heat exchanger coupled with thermoelectric cooler. *Int. J. Heat Mass Tran.* **2016**, *103*, 1084–1097. [[CrossRef](#)]
249. Nimmagadda, R.; Venkatasubbaiah, K. Experimental and multiphase analysis of nanofluids on the conjugate performance of micro-channel at low Reynolds numbers. *Heat Mass Tran.* **2017**, *53*, 2099–2115. [[CrossRef](#)]
250. Ho, C.; Liu, Y.; Ghalambaz, M.; Yan, W. Forced convection heat transfer of Nano-Encapsulated Phase Change Material (NEPCM) suspension in a mini-channel heatsink. *Int. J. Heat Mass Tran.* **2020**, *155*, 119858. [[CrossRef](#)]
251. Kumar, V.; Sarkar, J. Effect of different nanoparticles mixture dispersed nanofluids on hydrothermal characteristics in mini channel heat sink. *Adv. Powder Technol.* **2020**, *31*, 621–631. [[CrossRef](#)]
252. Nimmagadda, R.; Venkatasubbaiah, K. Two-phase analysis on the conjugate heat transfer performance of microchannel with Cu, Al, SWCNT, and hybrid nanofluids. *J. Therm. Sci. Eng. Appl.* **2017**, *9*, 041011. [[CrossRef](#)]
253. Bahiraei, M.; Berahmand, M.; Shahsavari, A. Irreversibility analysis for flow of a non Newtonian hybrid nanofluid containing coated CNT/Fe₃O₄ nanoparticles in a mini channel heat exchanger. *Appl. Therm. Eng.* **2017**, *125*, 1083–1093. [[CrossRef](#)]
254. Mashayekhi, R.; Khodabandeh, E.; Akbari, O.; Toghraie, D.; Bahiraei, M.; Gholami, M. CFD analysis of thermal and hydrodynamic characteristics of hybrid nanofluid in a new designed sinusoidal double-layered microchannel heat sink. *J. Therm. Anal. Calorim.* **2018**, *134*, 2305–2315. [[CrossRef](#)]
255. Bahiraei, M.; Jamshidmofid, M.; Dahari, M. Second law analysis of hybrid nanofluid flow in a microchannel heat sink integrated with ribs and secondary channels for utilization in miniature thermal devices. *Chem. Eng. Process* **2020**, *153*, 107963. [[CrossRef](#)]
256. Ho, C.; Guo, Y.; Yang, T.; Rashidi, S.; Yan, W. Numerical study on forced convection of water-based suspensions of nanoencapsulated PCM particles/Al₂O₃ nanoparticles in a mini-channel heat sink. *Int. J. Heat Mass Tran.* **2020**, *157*, 119965. [[CrossRef](#)]
257. Uysal, C.; Gedik, E.; Chamkha, A. A Numerical analysis of laminar forced convection and entropy generation of a diamond-Fe₃O₄/water hybrid nanofluid in a rectangular mini channel. *J. Appl. Fluid Mech.* **2019**, *12*, 391–402. [[CrossRef](#)]
258. Shahsavari, A.; Godini, A.; Sardari, P.; Toghraie, D.; Salehipour, H. Impact of variable fluid properties on forced convection of Fe₃O₄/CNT/water hybrid nanofluid in a double-pipe mini-channel heat exchanger. *J. Therm. Anal. Calorim.* **2019**, *137*, 1031–1043. [[CrossRef](#)]
259. He, W.; Mashayekhi, R.; Toghraie, D.; Akbari, O.; Li, Z.; Tlili, I. Hydrothermal performance of nanofluid flow in a sinusoidal double layer microchannel in order to geometric optimization. *Int. Commun. Heat Mass Tran.* **2020**, *117*, 104700. [[CrossRef](#)]
260. Pantzali, M.N.; Kanaris, A.G.; Antoniadis, K.D.; Mouza, A.A.; Paras, S.V. Effect of nanofluids on the performance of a miniature plate heat exchanger with modulated surface. *Int. J. Heat Fluid Flow* **2009**, *30*, 691–699. [[CrossRef](#)]
261. Gherasim, I.; Galanis, N.; Nguyen, C.T. Numerical study of nanofluid flow and heat transfer in a plate heat exchanger. *Comput. Therm.* **2013**, *5*, 317–332. [[CrossRef](#)]

262. Ray, D.R.; Das, D.K.; Vajjha, R.S. Experimental and numerical investigations of nanofluids performance in a compact minichannel plate heat exchanger. *Int. J. Heat Mass Transf.* **2014**, *71*, 732–746. [[CrossRef](#)]
263. Tiwari, A.K.; Ghosh, P.; Sarkar, J.; Dahiya, H.; Parekh, J. Numerical investigation of heat transfer and fluid flow in plate heat exchanger using nanofluids. *Int. J. Therm. Sci.* **2014**, *85*, 93–103. [[CrossRef](#)]
264. Stogiannis, I.A.; Mouza, A.A.; Paras, S.V. Efficacy of SiO₂ nanofluids in a miniature plate heat exchanger with undulated surface. *Int. J. Therm. Sci.* **2015**, *92*, 230–238. [[CrossRef](#)]
265. Jokar, A.; O'Halloran, S.P. Heat transfer and fluid flow analysis of nanofluids in corrugated plate heat exchangers using computational fluid dynamics simulation. *J. Therm. Sci. Eng. Appl.* **2013**, *5*, 011002. [[CrossRef](#)]
266. Goodarzi, M.; Amiri, A.; Goodarzi, M.S.; Safaei, M.R.; Karimipour, A.; Languri, E.M.; Dahari, M. Investigation of heat transfer and pressure drop of a counter flow corrugated plate heat exchanger using MWCNT based nanofluids. *Int. Commun. Heat Mass Transf.* **2015**, *66*, 172–179. [[CrossRef](#)]
267. Bhattad, A.; Sarkar, J.; Ghosh, P. Discrete phase numerical model and experimental study of hybrid nanofluid heat transfer and pressure drop in plate heat exchanger. *Int. Commun. Heat Mass Transf.* **2018**, *91*, 262–273. [[CrossRef](#)]
268. Ding, Z.; Qi, C.; Luo, T.; Wang, Y.; Tu, J.; Wang, C. Numerical simulation of nanofluids forced convection in a corrugated double-pipe heat exchanger. *Can. J. Chem. Eng.* **2021**, *100*, 1954–1964. [[CrossRef](#)]
269. Bhattad, A.; Babu, S.S. Thermal analysis of shell and tube type heat exchanger using hybrid nanofluid. *Trends Sci.* **2022**, *19*, 2890. [[CrossRef](#)]
270. Jafarmadar, S.; Azizinia, N.; Razmara, N.; Mobadersani, F. Thermal analysis and entropy generation of pulsating heat pipes using nanofluids. *Appl. Therm. Eng.* **2016**, *103*, 356–364. [[CrossRef](#)]
271. Yan, H.; Yang, J.; Zhang, W. Numerical study of enhanced heat transfer of microchannel heat sink with nanofluids. *IOP Conf. Ser. Mater. Sci. Eng.* **2020**, *721*, 012052.
272. Khetib, Y.; Abo-Dief, H.M.; Alanazi, A.K.; Sajadi, S.M.; Sharifpur, M.; Meyer, J.P. A computational fluid dynamic study on efficiency of a wavy microchannel/heat sink containing various nanoparticles. *Micromachines* **2021**, *12*, 1192. [[CrossRef](#)]
273. Kalteh, M.; Kouhikamali, R.; Akbari, S. Numerical simulation of nanofluid heat transfer in a double-layered microchannel heat sink using two phase mixture model. *J. Nanofluids* **2016**, *5*, 139–147. [[CrossRef](#)]
274. Pantzali, M.N.; Mouza, A.A.; Paras, S.V. Investigating the efficacy of nanofluids as coolants in plate heat exchangers (PHE). *Chem. Eng. Sci.* **2009**, *64*, 3290–3300. [[CrossRef](#)]
275. Zamzadian, A.; Oskouie, S.N.; Doosthoseini, A.; Joneidi, A.; Pazouki, M. Experimental investigation of forced convective heat transfer coefficient in nanofluids of Al₂O₃/EG and CuO/EG in a double pipe and plate heat exchangers under turbulent flow. *Exp. Therm. Fluid Sci.* **2011**, *35*, 495–502. [[CrossRef](#)]
276. Kabeel, A.E.; El-Maaty, T.M.A.; El-Samadony, Y. The effect of using nano-particles on corrugated plate heat exchanger performance. *Appl. Therm. Eng.* **2013**, *52*, 221–229. [[CrossRef](#)]
277. Tiwari, A.K.; Ghosh, P.; Sarkar, J. Heat transfer and pressure drop characteristics of CeO₂/water nanofluid in plate heat exchanger. *Appl. Therm. Eng.* **2013**, *57*, 24–32. [[CrossRef](#)]
278. Khairul, M.A.; Alim, M.A.; Mahbulul, I.M.; Saidur, R.; Hepbasli, A.; Hossain, A. Heat transfer performance and exergy analyses of a corrugated plate heat exchanger using metal oxide nanofluids. *Int. Commun. Heat Mass Transf.* **2014**, *50*, 8–14. [[CrossRef](#)]
279. Huang, D.; Wu, Z.; Sunden, B. Effects of hybrid nanofluid mixture in plate heat exchangers. *Exp. Therm. Fluid Sci.* **2016**, *72*, 190–196. [[CrossRef](#)]
280. Tabari, Z.T.; Heris, S.Z. Heat Transfer Performance of Milk Pasteurization Plate Heat Exchangers Using MWCNT/Water Nanofluid. *J. Dispers. Sci. Technol.* **2015**, *36*, 196–204. [[CrossRef](#)]
281. Abed, A.M.; Alghoul, M.A.; Sopian, K.; Mohammed, H.A.; Al-Shamani, A.N. Design characteristics of corrugated trapezoidal plate heat exchangers using nanofluids. *Chem. Eng. Process. Process Intensif.* **2015**, *87*, 88–103. [[CrossRef](#)]
282. Behrangzade, A.; Heyhat, M.M. The effect of using nano-silver dispersed water based nanofluid as a passive method for energy efficiency enhancement in a plate heat exchanger. *Appl. Therm. Eng.* **2016**, *102*, 311–317. [[CrossRef](#)]
283. Sarafraz, M.M.; Hormozi, F.J.E.T. Heat transfer, pressure drop and fouling studies of multi-walled carbon nanotube nanofluids inside a plate heat exchanger. *Exp. Therm. Fluid Sci.* **2016**, *72*, 1–11. [[CrossRef](#)]
284. Sun, P.; Zuo, Y. Investigation on the flow and convective heat transfer characteristics of nanofluids in the plate heat exchanger. *Exp. Therm. Fluid Sci.* **2016**, *76*, 75–86. [[CrossRef](#)]
285. Kumar, V.; Tiwari, A.K.; Ghosh, S.K. Effect of chevron angle on heat transfer performance in plate heat exchanger using ZnO/water nanofluid. *Energy Convers. Manag.* **2016**, *118*, 142–154. [[CrossRef](#)]
286. Kumar, V.; Tiwari, A.K.; Ghosh, S.K. Effect of variable spacing on performance of plate heat exchanger using nanofluids. *Energy* **2016**, *114*, 1107–1119. [[CrossRef](#)]
287. Ahmed, H.E.; Ahmed, M.I.; Seder, I.M.; Salman, B.H. Experimental investigation for sequential triangular double-layered microchannel heat sink with nanofluids. *Int. Commun. Heat Mass Transf.* **2016**, *77*, 104–115. [[CrossRef](#)]
288. Sarvar-Ardeh, S.; Rafee, R.; Rashidi, S. Hybrid nanofluids with temperature-dependent properties for use in double-layered microchannel heat sink; hydrothermal investigation. *J. Taiwan Inst. Chem. Eng.* **2021**, *124*, 53–62. [[CrossRef](#)]
289. Wang, J.; Yu, K.; Ye, M.; Wang, E.; Wang, W.; Sundén, B. Effects of pin fins; vortex generators on thermal performance in a microchannel with Al₂O₃ nanofluids. *Energy* **2022**, *239*, 122606. [[CrossRef](#)]

290. Adio, S.A.; Alo, T.A.; Olagoke, R.O.; Olalere, A.E.; Veeredhi, V.R.; Ewim, D.R. Thermohydraulic and entropy characteristics of Al_2O_3 -water nanofluid in a ribbed interrupted microchannel heat exchanger. *Heat Transf.* **2021**, *50*, 1951–1984. [[CrossRef](#)]
291. Adio, A.S.; Olalere, A.E.; Olagoke, R.O.; Alo, T.A.; Veeredhi, V.R.; Ewim, D.R.; Olakoyejo, O.T. Thermal and entropy analysis of a manifold microchannel heat sink operating on CuO -water nanofluid. *J. Braz. Soc. Mech. Sci. Eng.* **2021**, *43*, 1–15. [[CrossRef](#)]
292. Ali, M.A.; Angelino, M.; Rona, A. Numerical analysis on the thermal performance of microchannel heat sinks with Al_2O_3 nanofluid and various fins. *Appl. Therm. Eng.* **2021**, *198*, 117458. [[CrossRef](#)]
293. Kumar, M.P.; Kumar, C.A. Numerical study on heat transfer performance using Al_2O_3 /water nanofluids in six circular channel heat sink for electronic chip. *Mater. Today Proc.* **2020**, *21*, 194–201. [[CrossRef](#)]
294. Elbadawy, I.; Fayed, M. Reliability of Al_2O_3 nanofluid concentration on the heat transfer augmentation and resizing for single and double stack microchannels. *Alex. Eng. J.* **2020**, *59*, 1771–1785. [[CrossRef](#)]
295. Mostafa, K. Simulation of nanofluid flow through rectangular microchannel by modified thermal dispersion model. *Heat Transf. Eng.* **2020**, *41*, 377–392.
296. Pourfattah, F.; Arani, A.A.A.; Babaie, M.R.; Nguyen, H.M.; Asadi, A. On the thermal characteristics of a manifold microchannel heat sink subjected to nanofluid using two-phase flow simulation. *Int. J. Heat Mass Transf.* **2019**, *143*, 118518. [[CrossRef](#)]
297. Kumar, A.; Nath, S.; Bhanja, D. Effect of nanofluid on thermo hydraulic performance of double layer tapered microchannel heat sink used for electronic chip cooling. *Numer. Heat Transf. Part A Appl.* **2018**, *73*, 429–445. [[CrossRef](#)]
298. Arjun, K.S.; Rakesh, K. CFD analysis of thermal performance of microchannel nanofluid flow at different Reynolds numbers. *Songklanakar J. Sci. Technol.* **2019**, *41*, 109–116.
299. Madhava Reddy, H.; Venu Vinod, A. CFD simulation of the heat transfer using nanofluids in microchannel with dimple and protrusion. *Indian Chem. Eng.* **2019**, *61*, 40–51. [[CrossRef](#)]
300. Darzi, A.A.R.; Farhadi, M.; Sedighi, K. Heat transfer and flow characteristics of Al_2O_3 -water nanofluid in a double tube heat exchanger. *Int. Commun. Heat Mass Transf.* **2013**, *47*, 105–112. [[CrossRef](#)]
301. Maddah, H.; Alizadeh, M.; Ghasemi, N.; Alwi, S.R.W. Experimental study of Al_2O_3 /water nanofluid turbulent heat transfer enhancement in the horizontal double pipes fitted with modified twisted tapes. *Int. J. Heat Mass Transf.* **2014**, *78*, 1042–1054. [[CrossRef](#)]
302. Sarafraz, M.M.; Hormozi, F. Intensification of forced convection heat transfer using biological nanofluid in a double-pipe heat exchanger. *Exp. Therm. Fluid Sci.* **2015**, *66*, 279–289. [[CrossRef](#)]
303. Jafarimoghaddam, A.; Aberoumand, S.; Aberoumand, H.; Javaherdeh, K. Experimental study on Cu /Oil nanofluids through concentric annular tube: A correlation. *Heat Tran. Asian Res.* **2017**, *46*, 251–260. [[CrossRef](#)]
304. Shirvan, K.M.; Mamourian, M.; Mirzakhani, S.; Ellahi, R. Numerical investigation of heat exchanger effectiveness in a double pipe heat exchanger filled with nanofluid: A sensitivity analysis by response surface methodology. *Powder Technol.* **2017**, *313*, 99–111. [[CrossRef](#)]
305. Akyurek, E.F.; Gelis, K.; Sahin, B.; Many, E. Experimental analysis for heat transfer of nanofluid with wire coil turbulators in a concentric tube heat exchanger. *Results Phys.* **2018**, *9*, 376–389. [[CrossRef](#)]
306. Albadr, J.; Tayal, S.; Alasadi, M. Heat transfer through heat exchanger using Al_2O_3 nanofluid at different concentrations. *Case Stud. Therm. Eng.* **2013**, *1*, 38–44. [[CrossRef](#)]
307. Godson, L.; Deepak, K.; Enoch, C.; Jefferson, B.; Raja, B. Heat transfer characteristics of silver/water nanofluids in a shell and tube heat exchanger. *Arch. Civ. Mech. Eng.* **2014**, *14*, 489–496. [[CrossRef](#)]
308. Dharmalingam, R.; Sivagnanaprabhu, K.K.; Yogaraja, J.; Gunasekaran, S.; Mohan, R. Experimental investigation of heat transfer characteristics of nanofluid using parallel flow, counter flow and shell and tube heat exchanger. *Arch. Mech. Eng.* **2015**, *LXII*, 509–522. [[CrossRef](#)]
309. Aghabozorg, M.H.; Rashidi, A.; Mohammadi, S. Experimental investigation of heat transfer enhancement of Fe_2O_3 -CNT/water magnetic nanofluids under laminar, transient and turbulent flow inside a horizontal shell and tube heat exchanger. *Exp. Therm. Fluid Sci.* **2016**, *72*, 182–189. [[CrossRef](#)]
310. Tan, Y.; He, Z.; Xu, T.; Fang, X.; Gao, X.; Zhang, Z. Experimental investigation of heat transfer and pressure drop characteristics of non-Newtonian nanofluids flowing in the shell-side of a helical baffle heat exchanger with low-finned tubes. *Heat Mass Transf.* **2017**, *53*, 2813–2827. [[CrossRef](#)]
311. Naik, B.A.K.; Vinod, A.V. Heat transfer enhancement using non Newtonian nanofluids in a shell and helical coil heat exchanger. *Exp. Therm. Fluid Sci.* **2018**, *90*, 132–142. [[CrossRef](#)]
312. Said, Z.; Rahman, S.M.A.; Assad, M.E.H.; Alami, A.H. Heat transfer enhancement and life cycle analysis of a Shell-and-Tube Heat Exchanger using stable CuO /water nanofluid. *Sustain. Energy Technol. Assessm.* **2019**, *31*, 306–317. [[CrossRef](#)]
313. Arshad, M.; Hussain, A.; Hassan, A.; Wro, P.; Elfakhany, A.; Elkotb, M.; Abdelmohimen, M.; Galal, A. Thermal energy investigation of magnetohydrodynamic nano-material liquid flow over a stretching sheet: Comparison of single and composite particles. *Alex. Eng. J.* **2022**, *61*, 10453–10462. [[CrossRef](#)]
314. Bhattad, A.; Sarkar, J.; Ghosh, P. Exergetic analysis of plate evaporator using hybrid nanofluids as secondary refrigerant for low temperature applications. *Int. J. Exergy* **2017**, *24*, 1–20. [[CrossRef](#)]
315. Bhattad, A.; Sarkar, J.; Ghosh, P. Energetic and exergetic performances of plate heat exchanger using brine based hybrid nanofluid for milk chilling application. *Heat Transf. Eng.* **2020**, *41*, 522–535. [[CrossRef](#)]

316. Mishra, R.; Das, P.K.; Sarangi, S. Second law based optimisation of crossflow plate-fin heat exchanger design using genetic algorithm. *Appl. Therm. Eng.* **2009**, *29*, 2983–2989. [[CrossRef](#)]
317. Rosen, M.A.; Dincer, I.; Kanoglu, M. Role of exergy in increasing efficiency and sustainability and reducing environmental impact. *Energy Pol.* **2008**, *36*, 128–137. [[CrossRef](#)]
318. Bejan, A. *Entropy Generation through Heat; Fluid Flow*; Wiley: New York, NY, USA, 1982.
319. Kumar, V.; Sahoo, R.R. Exergy and energy analysis of a wavy fin radiator with variously shaped nanofluids as coolants. *Heat Transfer. Asian Res.* **2019**, *48*, 2174–2192. [[CrossRef](#)]
320. Bahiraei, M.; Mazaheri, N.; Aliee, F. Second law analysis of a hybrid nanofluid in tubes equipped with double twisted tape inserts. *Powder Technol.* **2019**, *345*, 692–703. [[CrossRef](#)]
321. Bahiraei, M.; Heshmatian, S. Efficacy of a novel liquid block working with a nanofluid containing graphene nanoplatelets decorated with silver nanoparticles compared with conventional cpu coolers. *Appl. Therm. Eng.* **2017**, *127*, 1233–1245. [[CrossRef](#)]
322. Sundar, L.S.; Mouli, C.K.V.; Said, Z.; Sousa, A.C. Heat transfer and second law analysis of ethylene glycol-based ternary hybrid nanofluid under laminar flow. *ASME J. Therm. Sci. Eng. Appl.* **2021**, *13*, 051021. [[CrossRef](#)]
323. Mmohammadiun, M.; Dashtestani, F.; Alizadeh, M. Exergy prediction model of a double pipe heat exchanger using metal oxide nanofluids and twisted tape based on the artificial neural network approach and experimental results. *ASME J. Heat Transfer-Trans.* **2016**, *138*, 011801. [[CrossRef](#)]
324. Singh, S.K.; Sarkar, J. Improving hydrothermal performance of double-tube heat exchanger with modified twisted tape inserts using hybrid nanofluid. *J. Therm. Anal. Calorim.* **2021**, *143*, 4287–4298. [[CrossRef](#)]
325. Kumar, V.; Sahoo, R. Energy-economic and exergy-environment performance evaluation of compact heat exchanger with turbulator passive inserts using THDNF. *J. Therm. Sci. Eng. Appl.* **2023**, *15*, 021011. [[CrossRef](#)]
326. Kumar, V.; Sahoo, R. 4 E's (Energy, Exergy, Economic, Environmental) performance analysis of air heat exchanger equipped with various twisted turbulator inserts utilizing ternary hybrid nanofluids. *Alex. Eng. J.* **2022**, *61*, 5033–5050. [[CrossRef](#)]
327. Rai, R.; Sahoo, R. Experimental energetic and exergetic analysis with the novel emulsion fuels incorporating CNT and Al₂O₃ nano additive for DIC engine. *Int. J. Exergy* **2021**, *34*, 4492–4514. [[CrossRef](#)]
328. Saidur, R.; Kazi, S.N.; Hossain, M.S.; Rahman, M.M.; Mohammed, H.A. A review on the performance of nanoparticles suspended with refrigerants and lubricating oils in refrigeration systems. *Renew. Sustain. Energy Rev.* **2011**, *15*, 310–323. [[CrossRef](#)]
329. Bhattad, A.; Sarkar, J.; Ghosh, P. Improving the performance of refrigeration systems by using nanofluids: A comprehensive review. *Renew. Sustain. Energy Rev.* **2018**, *82*, 3656–3669. [[CrossRef](#)]
330. Alawi, O.A.; Sidik, N.A.C.; Mohammed, H.A. A comprehensive review of fundamentals, preparation and applications of nanorefrigerants. *Int. Commun. Heat Mass Transf.* **2014**, *54*, 81–95. [[CrossRef](#)]
331. Celen, A.; Çebi, A.; Aktas, M.; Mahian, O.; Dalkilic, A.S.; Wongwises, S. A review of nanorefrigerants: Flow characteristics and applications. *Int. J. Refrig.* **2014**, *44*, 125–140. [[CrossRef](#)]
332. Alawi, O.A.; Sidik, N.A.C. Applications of nanorefrigerant and nanolubricants in refrigeration, air-conditioning and heat pump systems: A review. *Int. Commun. Heat Mass Transf.* **2015**, *68*, 91–97. [[CrossRef](#)]
333. Alawi, O.A.; Sidik, N.A.C.; Kherbeet, A.S. Nanorefrigerant effects in heat transfer performance and energy consumption reduction: A review. *Int. Commun. Heat Mass Transf.* **2015**, *69*, 76–83. [[CrossRef](#)]
334. Patil, M.S.; Kim, S.C.; Seo, J.H.; Lee, M.Y. Review of the thermo-physical properties and performance characteristics of a refrigeration system using refrigerant-based nanofluids. *Energies* **2016**, *9*, 22. [[CrossRef](#)]
335. Nair, V.; Tailor, P.R.; Parekh, A.D. Nanorefrigerants: A comprehensive review on its past, present and future. *Int. J. Refrig.* **2016**, *67*, 290–307. [[CrossRef](#)]
336. Zawawi, N.N.M.; Azmi, W.H.; Redhwan, A.A.M.; Sharif, M.Z.; Sharma, K.V. Thermo-physical properties of Al₂O₃-SiO₂/PAG composite nanolubricant for refrigeration system. *Int. J. Refrig.* **2017**, *80*, 1–10. [[CrossRef](#)]
337. Fard, M.H.; Talaie, N. Numerical and experimental investigation of heat transfer of ZnO/Water nanofluid in the concentric tube and plate heat exchangers. *Therm. Sci.* **2011**, *1*, 183–194.
338. Javadi, F.S.; Sadeghipour, S.; Saisur, R.; Boroumandjazi, G.; Rahmati, B.; Elias, M.M.; Sohel, M.R. The effects of nanofluid on thermophysical properties and heat transfer characteristics of a plate heat exchanger. *Int. Commun. Heat Mass Transf.* **2013**, *44*, 58–63. [[CrossRef](#)]
339. Maré, T.; Halelfadl, S.; Sow, O.; Estellé, P.; Duret, S.; Bazantay, F. Comparison of the thermal performances of two nanofluids at low temperature in a plate heat exchanger. *Exp. Therm. Fluid Sci.* **2011**, *35*, 1535–1543. [[CrossRef](#)]
340. Nitsas, M.T.; Koronaki, I.P. Investigating the potential impact of nanofluids on the performance of condensers and evaporators-A general approach. *Appl. Therm. Eng.* **2016**, *100*, 577–585. [[CrossRef](#)]
341. Liu, M.S.; Lin, M.C.C.; Liaw, J.S.; Wang, C.C. Performance augmentation of a water chiller system using nanofluids. *ASHRAE Trans.* **2009**, *115*, 581–586.
342. Kumaresan, V.; Velraj, R.; Das, S.K. Convective heat transfer characteristics of secondary refrigerant based CNT nanofluids in a tubular heat exchanger. *Int. J. Refrig.* **2012**, *35*, 2287–2296. [[CrossRef](#)]
343. Loaiza, J.C.V.; Pruzaesky, F.C.; Parise, J.A.R. A numerical study on the application of nanofluids in refrigeration systems. In Proceedings of the 13th International Refrigeration and Air-Conditioning Conference at Purdue, West Lafayette, IN, USA, 12–15 July 2010; pp. 2495–2508.

344. Parise, J.A.R.; Tiecher, R.F.P. A simulation model for the application of nanofluids as condenser coolants in vapor compression heat pumps. In Proceedings of the 14th International Refrigeration and Air-Conditioning Conference at Purdue, West Lafayette, IN, USA, 16–19 July 2012; pp. 2531–2610.
345. Askari, S.; Lotfi, R.; Seifkordi, A.; Rashidi, A.M.; Koolivand, H. A novel approach for energy and water conservation in wet cooling towers by using MWNTs and nanoporous graphene nanofluids. *Energy Convers. Manag.* **2016**, *109*, 10–18. [[CrossRef](#)]
346. Kolhapure, K.B.; Patil, U.S. Experimental investigation of refrigeration system using Al_2O_3 /water nanofluids as cooling medium. *Int. J. Res. Aeronaut. Mech. Eng.* **2016**, *4*, 86–95.
347. Jaiswal, R.K.; Mishra, R.S. Performance evaluation of vapour compression refrigeration system using eco-friendly refrigerants in primary circuit and nanofluid (water- nano particles based) in secondary circuit. *Int. Res. J. Sustain. Sci. Eng.* **2014**, *2*, 350–362.
348. Ndoye, F.T.; Schalbart, P.; Leducq, D.; Alvarez, G. Numerical study of energy performance of nanofluids used in secondary loops of refrigeration systems. *Int. J. Refrig.* **2015**, *52*, 122–132. [[CrossRef](#)]
349. Soliman, A.M.A.; Abdelrahman, A.K.; Ookawara, S. Analytical investigation of energy performance in secondary loops of refrigeration systems using different nano materials additives. In Proceedings of the 15th International Conference on Sustainable Energy Technologies—SET, Singapore, 19–22 July 2016.
350. Vasconcelos, A.A.; Gómez, A.O.C.; Filho, E.P.B.; Parise, J.A.R. Experimental evaluation of SWCNT-water nanofluid as a secondary fluid in a refrigeration system. *Appl. Therm. Eng.* **2017**, *111*, 1487–1492. [[CrossRef](#)]
351. Zhai, X.Q.; Wang, X.L.; Wang, T.; Wang, R.Z. A review on phase change cold storage in AC system: Materials and applications. *Renew. Sustain. Energy Rev.* **2013**, *22*, 108–120. [[CrossRef](#)]
352. Hannon, J.C.; Kerry, J.; Cruz-Romero, M.; Morris, M.; Cummins, E. Advances and challenges for the use of engineered nanoparticles in food contact materials. *Trends Food Sci. Technol.* **2015**, *43*, 43–62. [[CrossRef](#)]
353. Zhang, X.J.; Qiu, L.M.; Zhang, X.B.; Tian, X.J. Analysis of the nucleation of nanofluids in the ice formation process. *Energy Convers. Manag.* **2010**, *51*, 130–134. [[CrossRef](#)]
354. Longo, G.A.; Righetti, G.; Zilio, C. Development of an innovative raw milk dispenser based on nanofluid technology. *Int. J. Food Eng.* **2016**, *12*, 165–172. [[CrossRef](#)]
355. Bhattad, A.; Sarkar, J.; Ghosh, P. Energy-Economic analysis of plate evaporator using brine based hybrid nanofluids as secondary refrigerant. *Int. J. Air Cond. Refrig.* **2018**, *26*, 1850003–1850012. [[CrossRef](#)]
356. Sarkar, J. Performance evaluation of using water-based nanofluids as coolants in the gas cooler of a transcritical CO_2 refrigerant system. *J. Enhanc. Heat Transf.* **2013**, *20*, 389–397. [[CrossRef](#)]
357. Sarkar, J. Performance improvement of double-tube gas cooler in CO_2 refrigeration system using nanofluids. *Therm. Sci.* **2015**, *19*, 109–118. [[CrossRef](#)]
358. Arshad, M.; Hussain, A.; Hassan, A.; Karamti, H.; Wro, P.; Khan, I.; Andualem, M.; Galal, A. Scrutinization of slip due to lateral velocity on the dynamics of engine oil conveying cupric and alumina nanoparticles subject to coriolis force. *Math. Probl. Eng.* **2022**, *2022*, 2526951. [[CrossRef](#)]
359. Kumar, V.; Sahoo, R. Experimental and numerical study on cooling system waste heat recovery for engine air preheating by ternary hybrid nanofluid. *J. Enhanc. Heat Transf.* **2021**, *28*, 1–29. [[CrossRef](#)]
360. Kumar, V.; Sahoo, R. Preheating Effects on Compression Ignition Engine Through Waste Heat Recovery Using THNF-Based Radiator Coolant: An Experimental Study. *J. Therm. Sci. Eng. Appl.* **2022**, *14*, 12. [[CrossRef](#)]
361. Rai, R.; Sahoo, R. Effect of CNT and Al_2O_3 -CNT hybrid nano-additive in water-emulsified fuels on DIC engine energetic and exergetic performances. *J. Therm. Anal. Calorim.* **2021**, *147*, 3577–3589. [[CrossRef](#)]
362. Najafi, G. Diesel engine combustion characteristics using Nanoparticles in biodiesel-diesel blends. *Fuel* **2018**, *212*, 668–678. [[CrossRef](#)]
363. Jiaqiang, E.; Zhang, Z.; Chen, J.; Pham, M.; Zhao, X.; Peng, Q.; Zhang, B.; Yin, Z. Performance and emission evaluation of a marine diesel engine fueled by water biodiesel-diesel emulsion blends with a fuel additive of a cerium oxide nano-particle. *Energy Convers. Manag.* **2018**, *169*, 194–205.
364. Kumar, N.; Raheman, H. Characterization of nano-oxide added water emulsified biodiesel blend prepared with optimal emulsifying parameters. *Renew. Energy* **2020**, *145*, 308–317. [[CrossRef](#)]
365. Wro, P. Investigation of energy losses of the internal combustion engine taking into account the correlation of the hydrophobic and hydrophilic. *Energy* **2023**, *264*, 126002. [[CrossRef](#)]
366. Wro, P. Reduction of friction energy in a piston combustion engine for hydrophobic and hydrophilic multilayer nanocoatings surrounded by soot. *Energy* **2023**, *271*, 126974. [[CrossRef](#)]
367. Rai, R.; Sahoo, R. Impact of different shape based hybrid nano additives in emulsion fuel for exergetic, energetic, and sustainability analysis of diesel engine. *Energy* **2020**, *214*, 119086. [[CrossRef](#)]
368. Rao, M.; Anand, R. Performance and emission characteristics improvement studies on biodiesel fuelled DIC engine using water and AIO (OH) nano-particles. *Appl. Therm. Eng.* **2016**, *98*, 636–645.
369. El-Seesy, A.; Attia, A.; El-Batsh, H. The effect of aluminum oxide nanoparticles addition with Jojoba methyl ester-diesel fuel blends on diesel engine performance, combustion, and emission characteristics. *Fuel* **2018**, *224*, 147–166. [[CrossRef](#)]
370. Ozcan, H. Energy and exergy analyses of Al_2O_3 -diesel-biodiesel blend in a diesel engine. *Int. J. Exergy* **2019**, *28*, 29–45. [[CrossRef](#)]

371. Hasannuddin, A.; Yahya, W.; Sarah, S.; Ithnin, A.; Syahrullail, S.; Sidik, N.; Kassim, K.; Ahmad, Y.; Hirofumi, N.; Ahmad, M.; et al. Nano-additives incorporated water in diesel emulsion fuel: Fuel properties, performance, and emission characteristics assessment. *Energy Convers. Manag.* **2018**, *169*, 291–314. [[CrossRef](#)]
372. Aghbashlo, M.; Tabatabaei, M.; Mohammadi, P.; Mirzajanzadeh, M.; Ardjmand, M.; Rashidi, A. Effect of an emission-reducing soluble hybrid nano-catalyst in diesel/biodiesel blends on exergetic performance of a DI diesel engine. *Renew. Energy* **2016**, *93*, 353–368. [[CrossRef](#)]

Disclaimer/Publisher’s Note: The statements, opinions and data contained in all publications are solely those of the individual author(s) and contributor(s) and not of MDPI and/or the editor(s). MDPI and/or the editor(s) disclaim responsibility for any injury to people or property resulting from any ideas, methods, instructions or products referred to in the content.